Supporting Information

Synthesis, Structures, and Conformational Characteristics of Pillararene-based Diels-Alder Adducts with Embedded Chiral Centres

Haiying Wang,[a] Tushar Ulhas Thikekar,[a,b] Jingfeng Xue,[b] Yumei Zhu,[a] Wangjian Fang,[a] Jiong Xu,[a] Andrew C.-H. Sue,[b,*] and Hongxia Zhao[a,*]

a. School of Pharmaceutical Science & Technology, Tianjin Key Laboratory for Modern Drug Delivery & High-Efficiency, Tianjin University, 92 Weijin Road, Nankai District, Tianjin 300072, P. R. China.

b. College of Chemistry and Chemical Engineering, Xiamen University, 422 Siming S Rd, Siming District, Xiamen, Fujian Province 361005, P. R. China.

* Corresponding E-mail address: andrewsue@xmu.edu.cn; zhaohongxia@tju.edu.cn.

Table of Contents

1. Materials and General Methods

Starting materials, reagents, and solvents were purchased from commercial vendors and used as received, unless otherwise noted. All reactions were performed under an Ar atmosphere and in dry solvents, unless otherwise stated. Analytical thin-layer chromatography (TLC) was performed on aluminum sheets, precoated with silica gel GF254. Flash column chromatography was performed over silica gel (200−300 mesh or 300−400 mesh). ^{1}H, ^{13}C and 2D NMR spectra were recorded on Bruker Avance 400 MHz and 600 MHz spectrometers at 298 K, unless otherwise noted. The chemical shifts are listed in ppm on the δ scale and coupling constants were recorded in Hertz (Hz). Chemical shifts are calibrated relative to the signals corresponding of the non-deuterated solvents ($CHCl_3$: δ 7.26 ppm for ^{1}H and 77.16 ppm for ^{13}C). The following abbreviations were used for multiplicities: s, singlet; d, doublet; t, triplet; m, multiplet or overlapping peaks; b, broad peaks. High-resolution mass spectra (HRMS) were measured on a Q-Exactive™ HF/UltiMate™ 3000 RSLCnano using a Nano ProFlow meter with ProFlow technology in positive mode. High-performance liquid chromatography (HPLC) analyses were operated using a LC-16A instrument (shimadzu corporation kyoto Japan). The separation was performed on a CHIRALPAK IE HPLC analytical column (5 μm, ID 4.6 mm × L 250 mm) purchased from Daicel Chemical Industries. The ECD spectra were recorded in the range 600 to 220 nm, a step size of 1.0 nm, a bandwidth of 2 nm on JASCO J-810 circular dichroism spectrometer at ambient conditions.

Single crystals suitable for X-ray diffraction were selected and mounted in inert oil in cold gas stream and their X-ray diffraction intensity data was collected on a Rigaku XtaLAB FRX diffractometer equipped with the Hypix6000HE detector, using Cu Kα radiation (λ = 1.54184 Å) and a Rigaku XtaLAB Synergy diffractometer equipped with the Hypix6000HE detector, using Mo Kα radiation (λ = 0.71073 Å). By the use of Olex2,[1] the structure was solved either (i) with the ShelXT structure solution program using Direct Methods or (ii) with the ShelXM structure solution program using Dual Space and (iii) refined with the ShelXL refinement package using Least Squares minimisation.[2] All non-hydrogen atoms were refined with anisotropic thermal parameters except the disordered carbon atoms. The hydrogen atoms were set in calculated positions and refined as riding atoms with a common fixed isotropic thermal parameter. Selected details of the data collection and structural refinement of each compound can be found within Table S1–S5 and full details are available in the corresponding CIF files. Crystallographic data (excluding structure factors) have been deposited with the Cambridge Crystallographic Data Centre and may be obtained free of charge via http://www.ccdc.cam.ac.uk/data_request/cif.

2. Synthetic Procedures

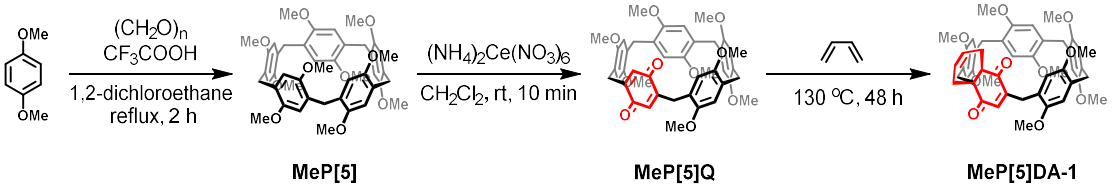

Scheme S1. Synthesis of **MeP[5]DA-1.**

MeP[5]: To a solution of 1,4-dimethoxybenzene (1.38 g, 10 mmol) and $(CH_2O)_n$ (0.30 g, 10 mmol) in 1,2-dichloroethane (100 mL), trifluoroacetic acid (5 mL) was added. The reaction mixture was refluxed for 2 h. After cooling, the reaction mixture was poured into methanol. The resulting precipitate of **MeP[5]** was collected by filtration. The crude product (1.20 g, 80%) was directly used in the following procedure without further purification.

MeP[5]Q: To a solution of **MeP[5]** (1.5 g, 2 mmol) in CH_2Cl_2 (200 mL) was added the solution of $(NH_4)_2Ce(NO_3)_6$ (2.2 g, 4 mmol) in water (2 mL) by dropwise, resulting in a red-coloured mixture which was stirred at 25 ℃ for 10 min. Water (100 mL) was added and the mixture was washed with copious amounts of water, the organic phase was dried over Na_2SO_4 and concentrated under reduced pressure. The residue was subjected to chromatography (EtOAc/*n*-hexane, 10/90) to afford the red solid product (840 mg, 60%). Data in accordance to literature.[3]

MeP[5]DA-1: MeP[5]Q (200 mg, 0.28 mmol) and 1,3-butadiene (1.9 mol/L in hexane, 10 mL, 19 mmol) was added into a dried Schlenk vessel with teflon-protected vacuum valve. The mixture was heated at 130 °C for 48 h. Upon cooling to room temperature, the reaction mixture was concentrated and purified by silica column chromatography (EtOAc/*n*-hexane, 2/5) and afford the product as yellow solid (88.9 mg, 41%). ^{1}H NMR (600 MHz, $CDCl_3$) δ 7.03 (s, 1H), 6.98 (s, 1H), 6.77 (s, 1H), 6.66 (s, 1H), 6.65 (s, 1H), 6.57 (s, 1H), 6.44 (s, 1H), 6.14 (d, J = 1.9 Hz, 1H), 5.66−5.58 (m, 2H), 5.07 (s, 1H), 3.96−3.89 (m, 4H), 3.88 (s, 1H), 3.81 (d, J = 13.6 Hz, 1H), 3.77 (m, 12H), 3.74 (s, 3H), 3.65 (d, J = 16.0 Hz, 1H), 3.61 (s, 3H), 3.48 (s, 3H), 3.24 (d, J = 15.7 Hz, 1H), 2.97 (d, J = 13.4 Hz, 1H), 2.91 (t, J = 7.5 Hz, 1H), 2.70 (d, J = 13.4 Hz, 1H), 2.40 (d, J = 18.0, 1H), 2.25−2.20 (m, 2H), 1.84 (d, J = 18.0 Hz, 1H), 1.76 (s, 3H). ^{13}C NMR (151 MHz, $CDCl_3$) δ 201.2, 199.9, 152.0, 151.2, 151.1, 151.1, 151.0, 150.5, 150.4, 147.3, 136.8, 130.3, 129.8, 129.6, 127.5, 126.5, 125.5, 124.5, 124.0, 121.3, 114.8, 114.1, 114.1, 114.1, 113.8, 113.6, 113.3, 111.1, 56.3, 56.2, 56.1, 56.0, 56.0, 55.9, 55.4, 52.7, 52.3, 51.9, 40.9, 30.8, 29.7, 29.4, 28.3, 26.4. HRMS (ESI) m/z $[M + NH_4]^+$ Calcd for $C_{47}H_{54}O_{10}N$ 792.3742, found 792.3732.

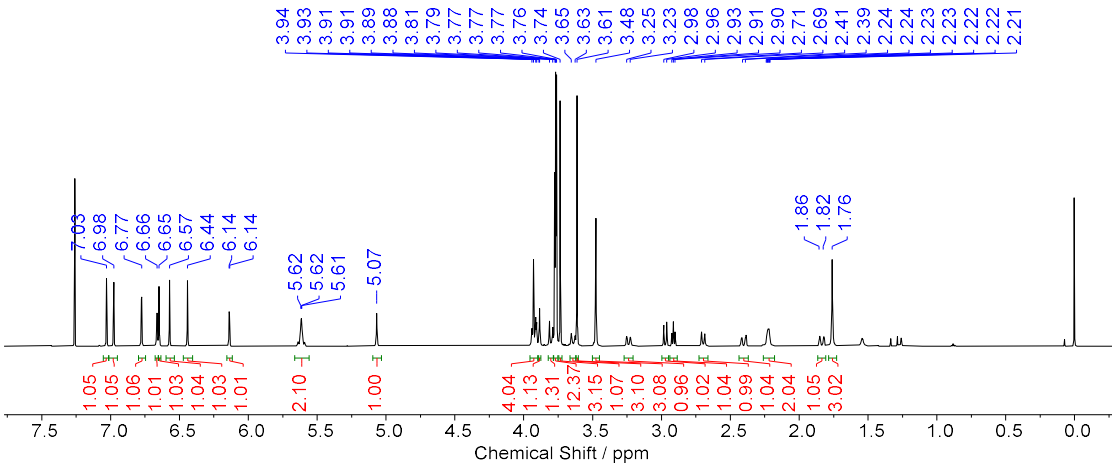

Fig. S1. ^{1}H NMR (600 MHz) spectrum of **MeP[5]DA-1** recorded in $CDCl_3$ at 298 K.

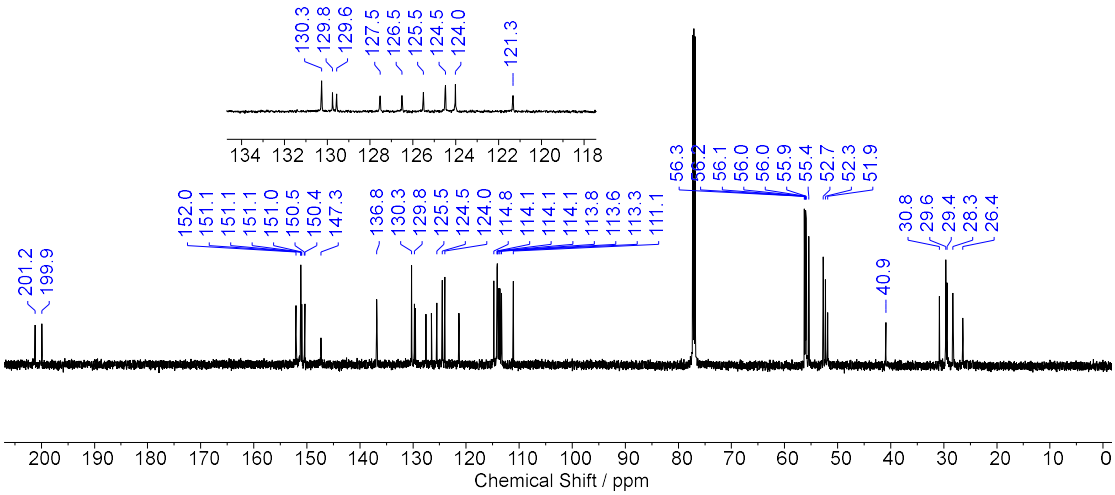

Fig. S2. ^{13}C NMR (150 MHz) spectrum of **MeP[5]DA-1** recorded in $CDCl_3$ at 298 K.

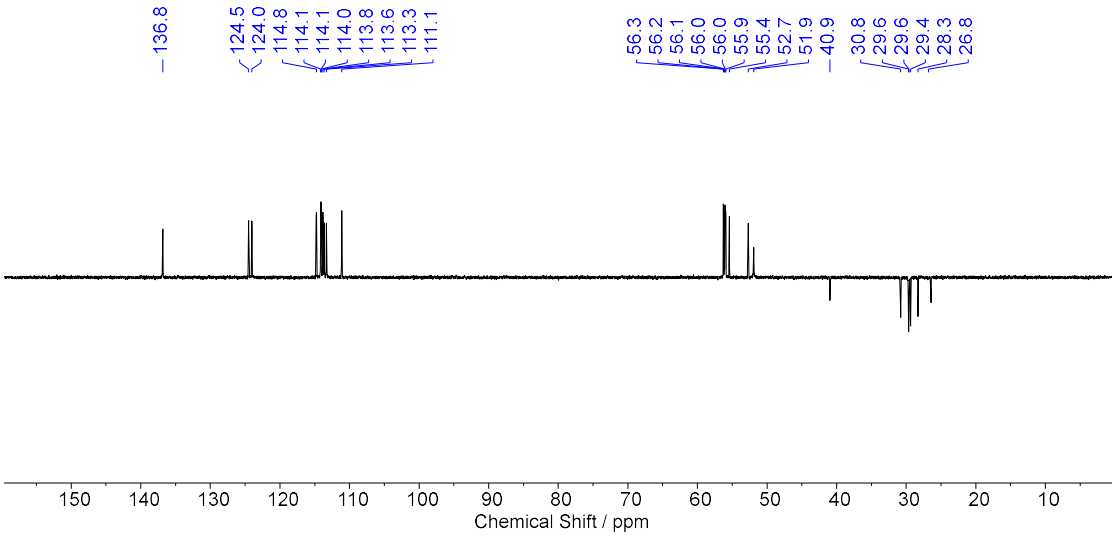

Fig. S3. DEPT 135° spectrum of **MeP[5]DA-1** recorded in $CDCl_3$ at 298 K.

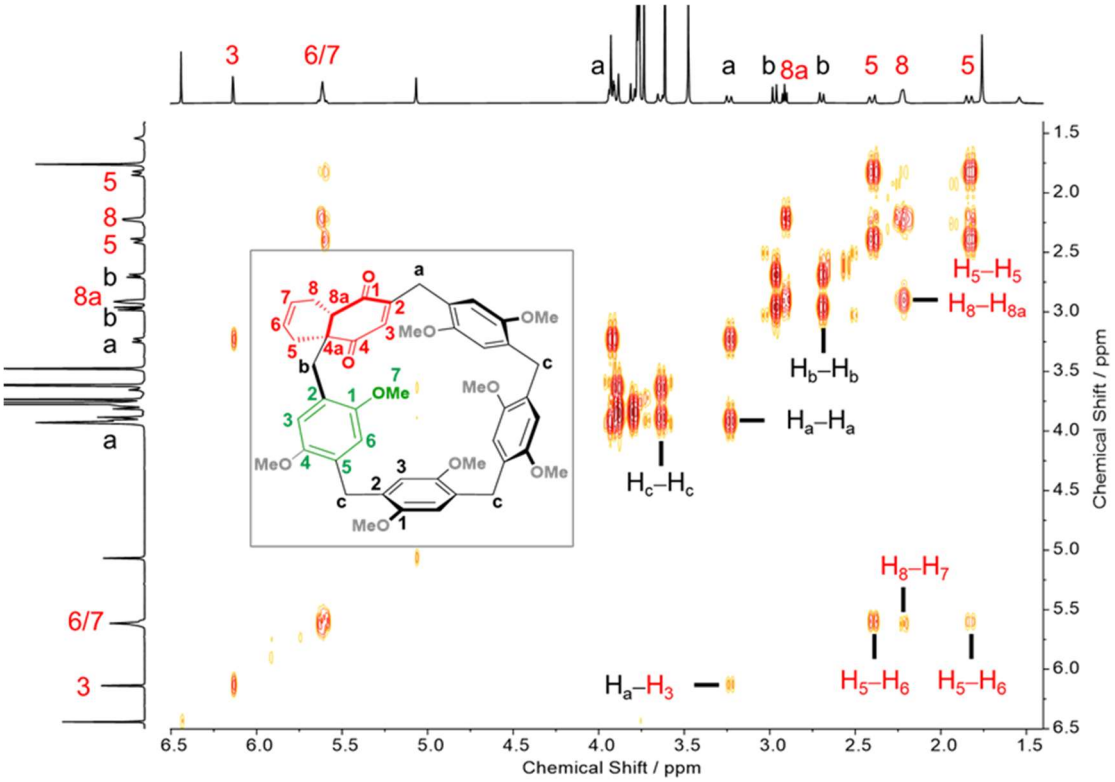

Fig. S4. ^{1}H–^{1}H COSY NMR spectrum of **MeP[5]DA-1** recorded in $CDCl_3$ at 298 K.

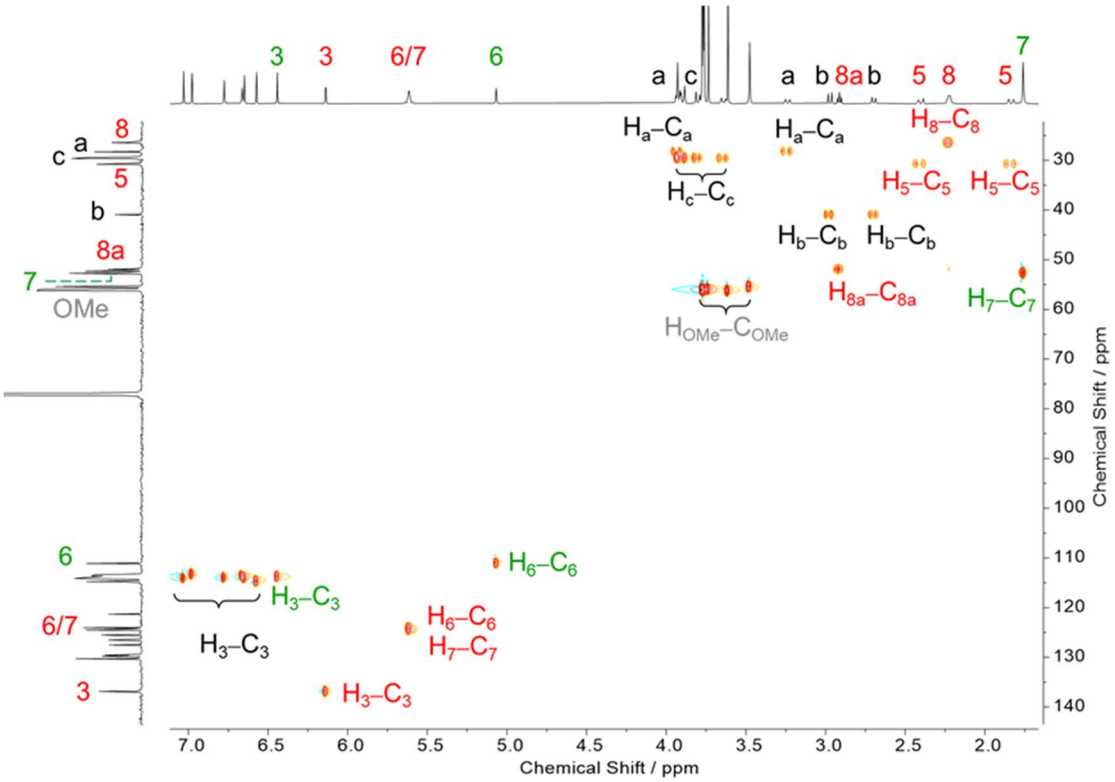

Fig. S5. ^{1}H–^{13}C HSQC NMR spectra of **MeP[5]DA-1** recorded in $CDCl_3$ at 298 K.

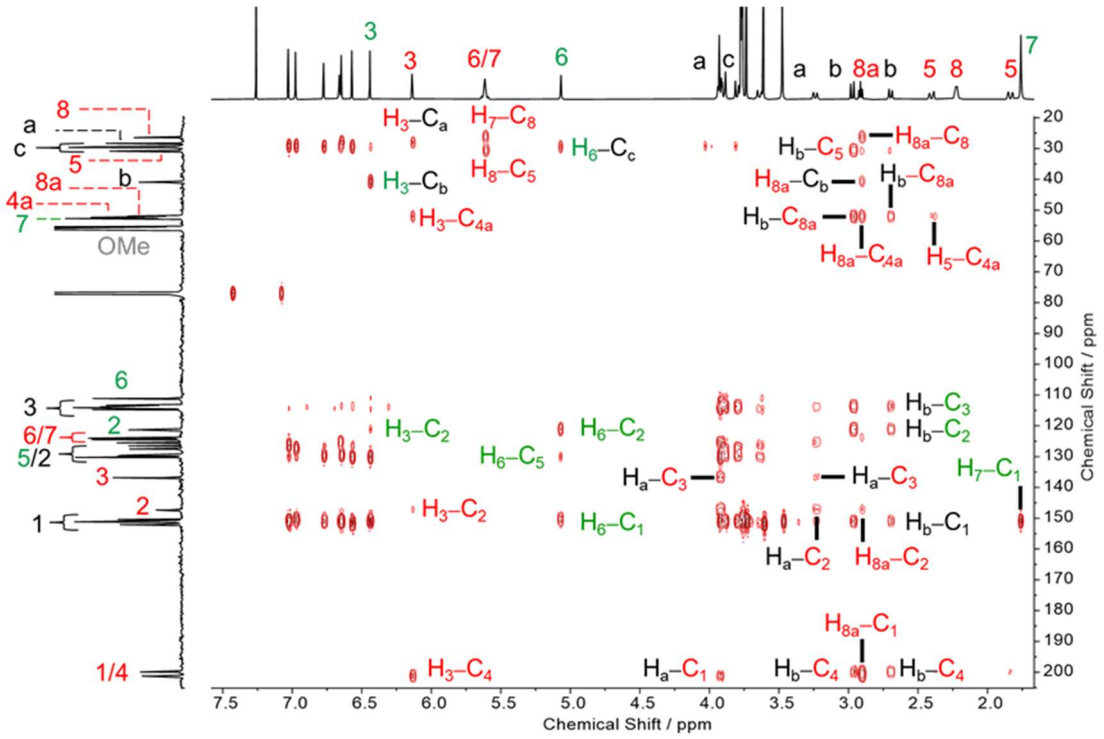

Fig. S6. $^{1}H–^{13}C$ HMBC NMR spectrum of **MeP[5]DA-1** recorded in $CDCl_3$ at 298 K.

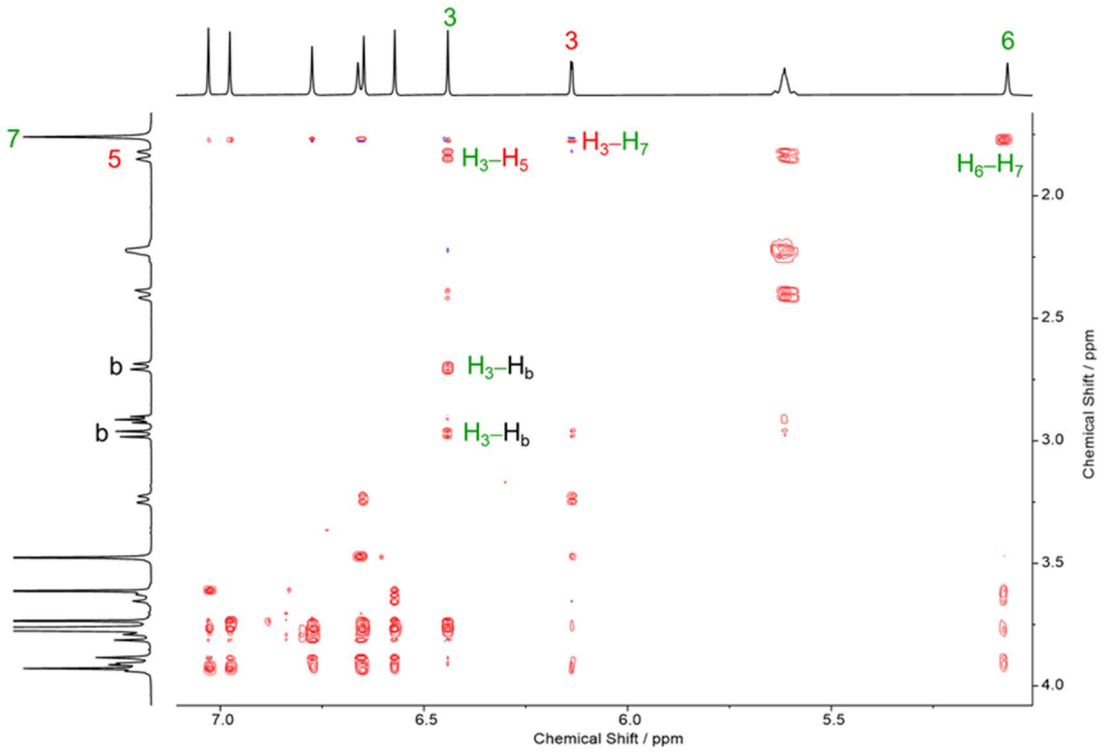

Fig. S7. $^{1}H–^{1}H$ ROESY NMR spectrum of **MeP[5]DA-1** recorded in $CDCl_3$ at 298 K.

MeP[5]DA-1: ^{1}H NMR (400 MHz, CD_3CN) δ 7.03 (s, 1H), 7.00 (s, 1H), 6.84 (s, 1H), 6.78 (s, 1H), 6.74 (s, 1H), 6.72 (s, 1H), 6.54 (s, 1H), 6.29 (s, 1H), 5.91 (s, 1H), 5.69−5.66 (m, 1H), 5.58−5.53 (m, 1H), 3.84−3.76 (m, 9H), 3.67 (s, 3H), 3.62 (s, 3H), 3.52 (s, 3H), 3.31 (d, J = 14.1 Hz, 1H), 2.96 (s, 2H), 2.63 (m, 4H), 2.34−2.25 (m, 1H), 2.24−2.08 (m, 3H), 1.91−1.82 (m, 1H). ^{13}C NMR (101 MHz, CD_3CN) δ 201.5, 200.5, 152.0, 151.7, 151.6, 151.2, 151.2, 151.1, 151.0, 149.5, 136.0, 130.1, 130.1, 129.7, 129.7, 128.5, 127.3, 125.5, 124.9, 123.9, 123.6, 117.9, 115.2, 115.0, 114.4, 114.1, 113.9, 113.8, 113.6, 113.2, 56.3, 56.1, 56.1, 56.0, 55.9, 55.9, 55.7, 54.43, 52.6, 50.3, 36.5, 32.6, 30.4, 29.5, 29.1, 29.0, 23.8.

(a)

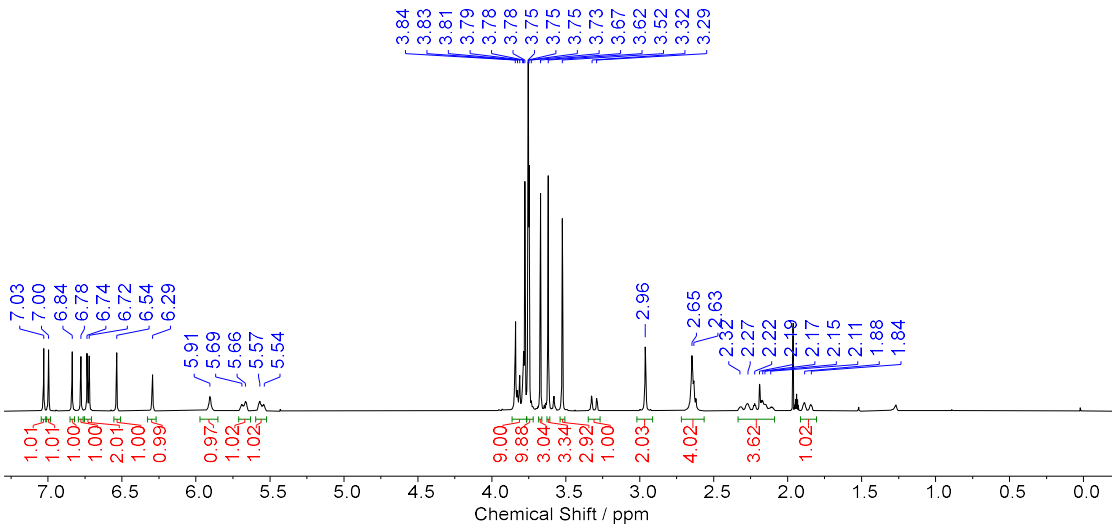

(b)

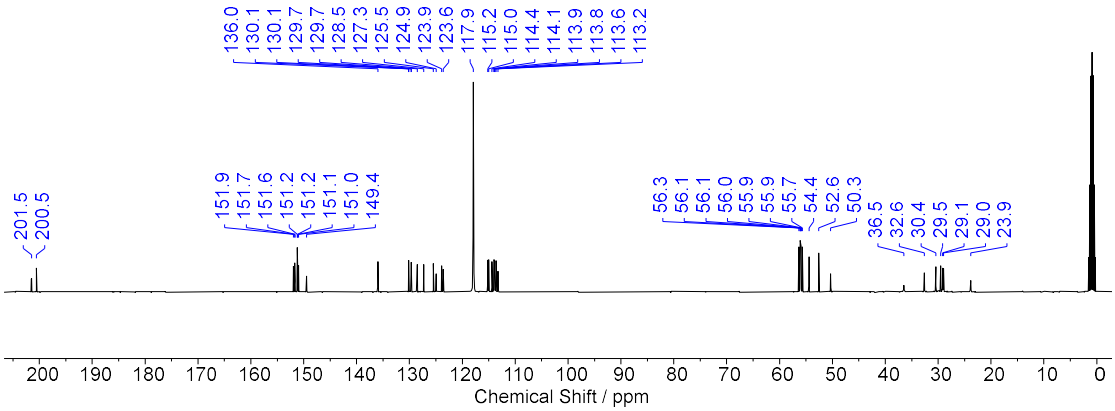

Fig. S8. (a) ^{1}H NMR (400 MHz) and (b) ^{13}C NMR (101 MHz) spectra of **MeP[5]DA-1** recorded in CD_3CN at 298 K.

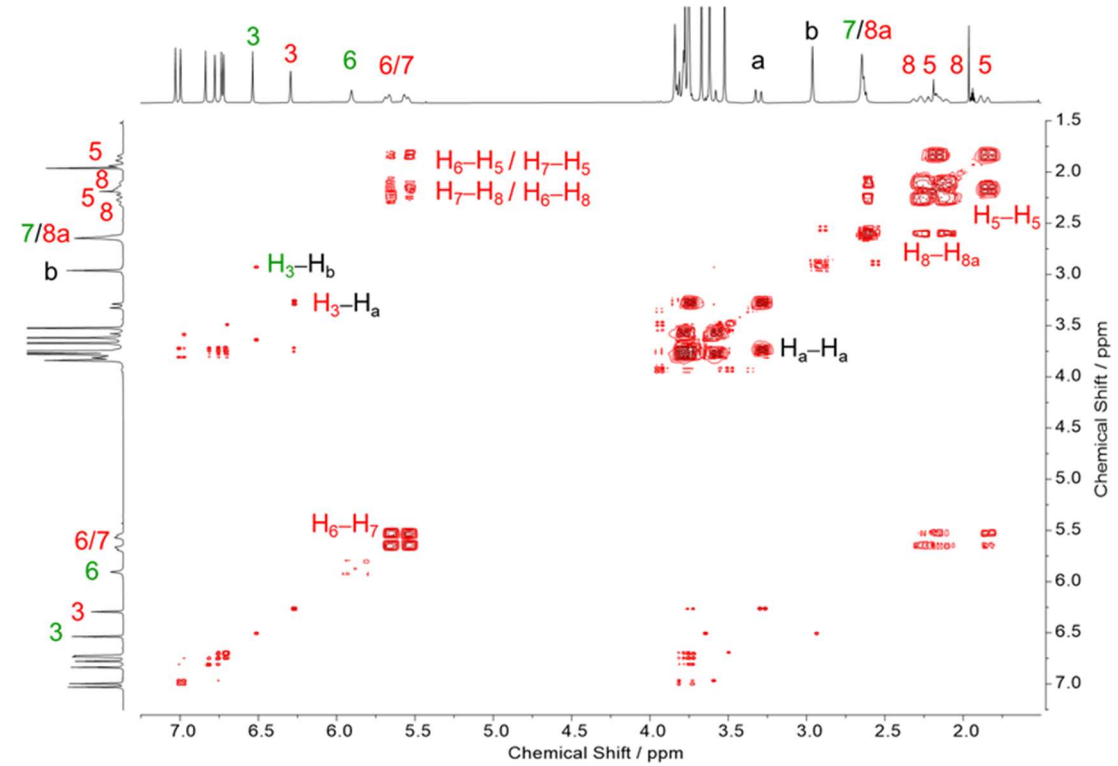

Fig. S9. ^{1}H–^{1}H COSY NMR spectrum of **MeP[5]DA-1** recorded in CD_3CN at 298 K.

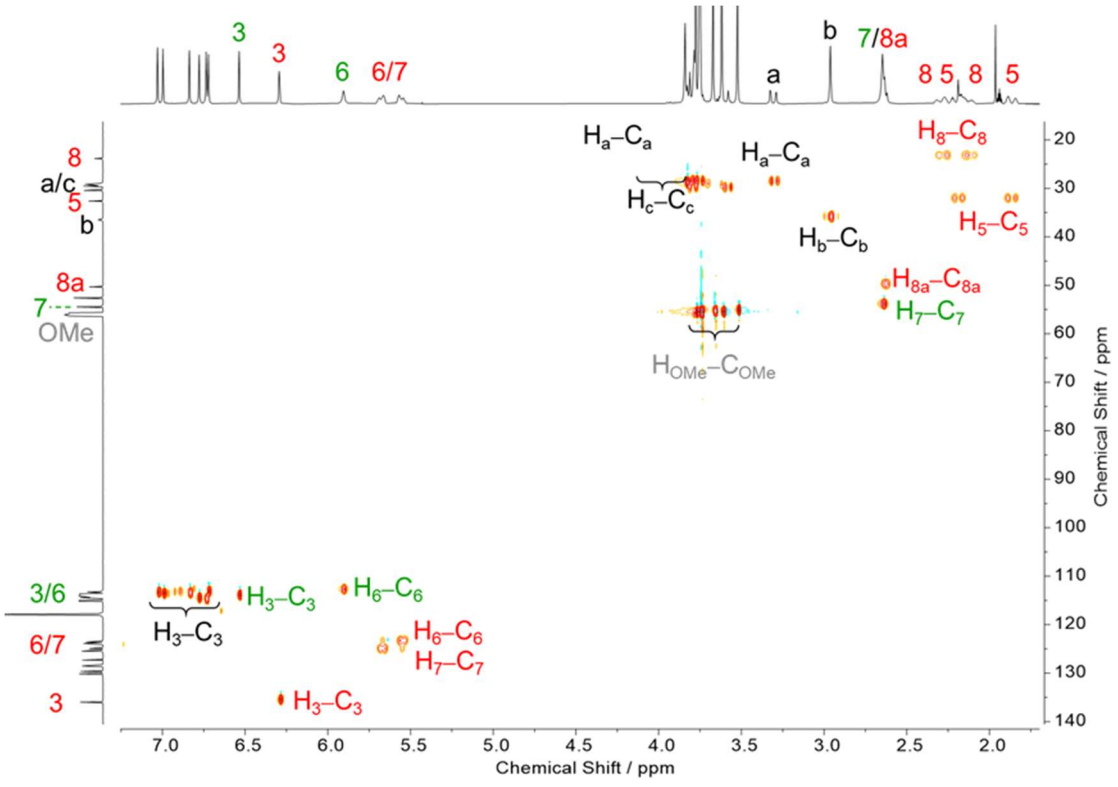

Fig. S10. ^{1}H–^{13}C HSQC NMR spectrum of **MeP[5]DA-1** recorded in CD_3CN at 298 K.

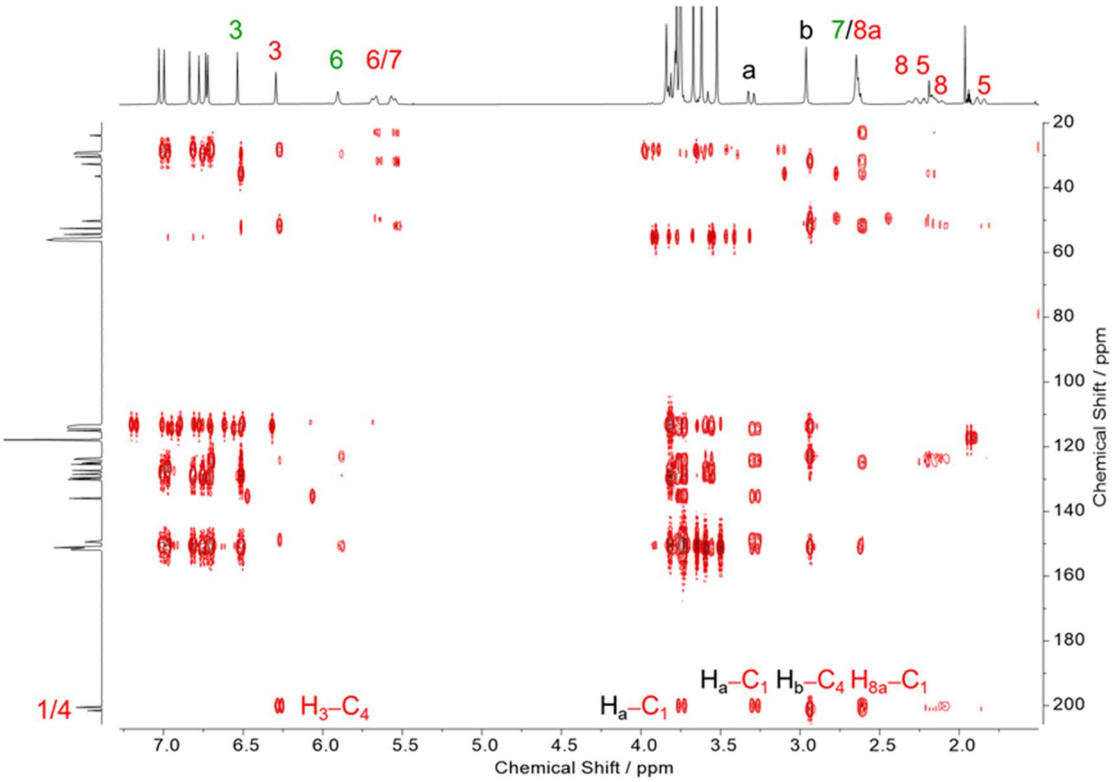

Fig. S11. $^{1}H–^{13}C$ HMBC NMR spectrum of **MeP[5]DA-1** recorded in CD_3CN at 298 K.

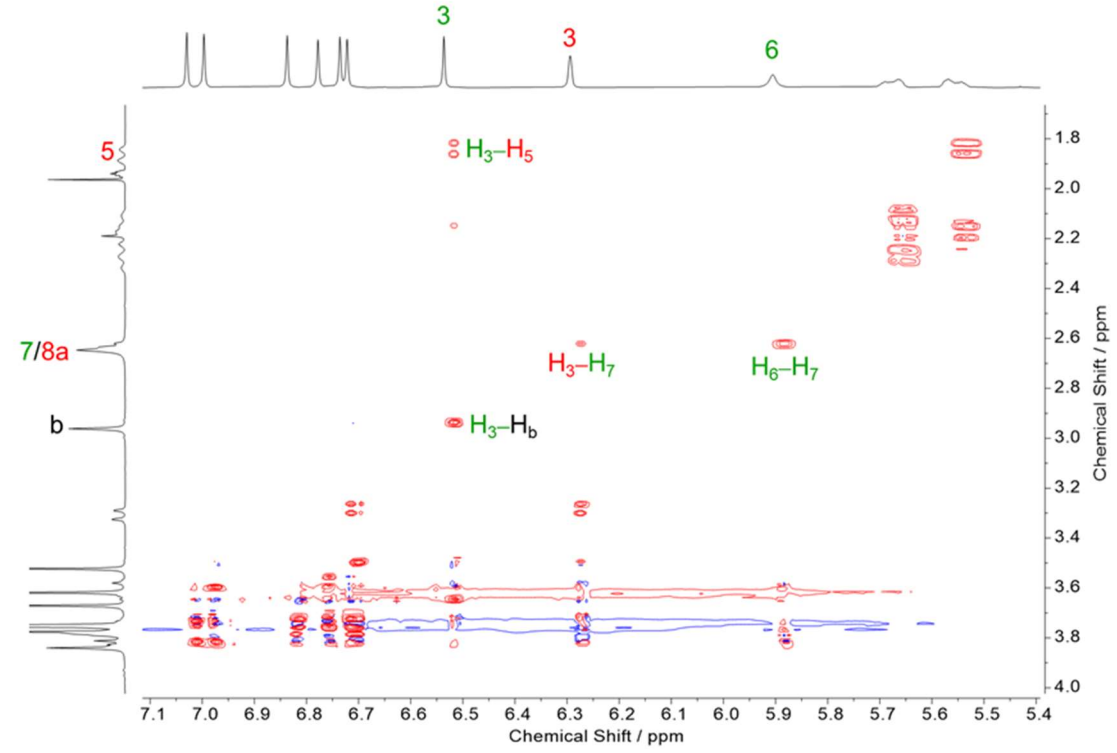

Fig. S12. $^{1}H–^{1}H$ ROESY NMR spectrum of **MeP[5]DA-1** recorded in CD_3CN at 298 K.

MeP[5]DA-1: ^{1}H NMR (400 MHz, d_6-DMSO) δ 7.01 (s, 1H), 6.96 (s, 1H), 6.85 (s, 1H), 6.80 (s, 1H), 6.71 (s, 1H), 6.60 (s, 2H), 5.96 (d, J = 2.0 Hz, 1H), 5.56−5.53 (m, 2H), 4.95 (s, 1H), 3.87−3.78 (m, 4H), 3.77−3.66 (m, 12H), 3.55 (s, 3H), 3.37 (s, 3H), 3.19 (d, J = 15.6 Hz, 1H), 2.84 (t, J = 7.6 Hz, 1H), 2.81−2.72 (m, 2H), 2.19−2.06 (m, 3H), 1.89 (d, J = 18.0 Hz, 1H), 1.67 (s, 3H). ^{13}C NMR (101 MHz, d_6-DMSO) δ 200.6, 199.2, 151.8, 151.0, 151.0, 150.9, 150.8, 150.5, 150.3, 147.4, 136.3, 130.0, 129.5, 129.4, 129.0, 127.4, 126.2, 125.9, 125.0, 124.2, 121.7, 115.3, 114.9, 114.2, 114.2, 113.8, 113.5, 113.4, 110.6, 56.5, 56.5, 56.4, 56.3, 56.2, 56.1, 55.6, 52.6, 52.0, 51.5, 30.3, 29.6, 29.4, 27.8, 26.4.

(a)

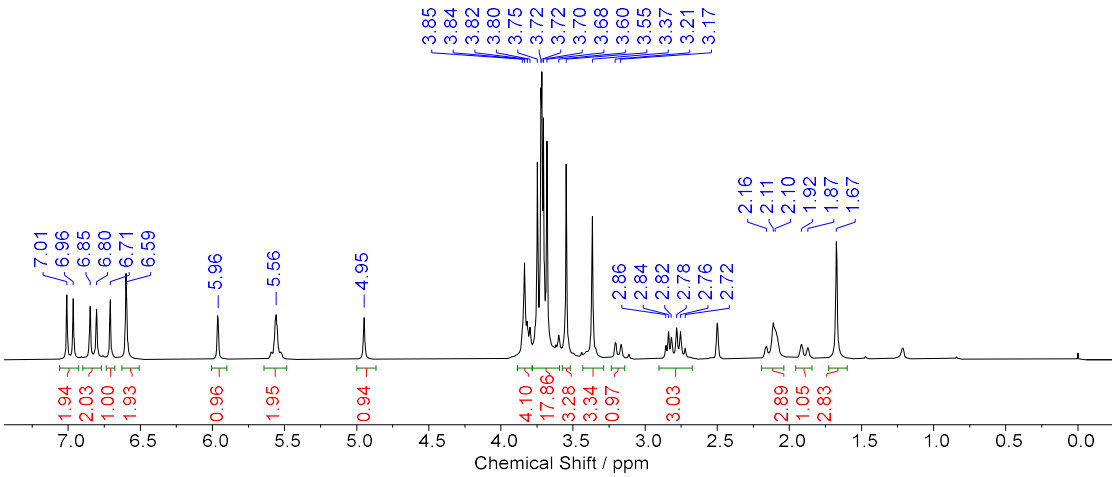

(b)

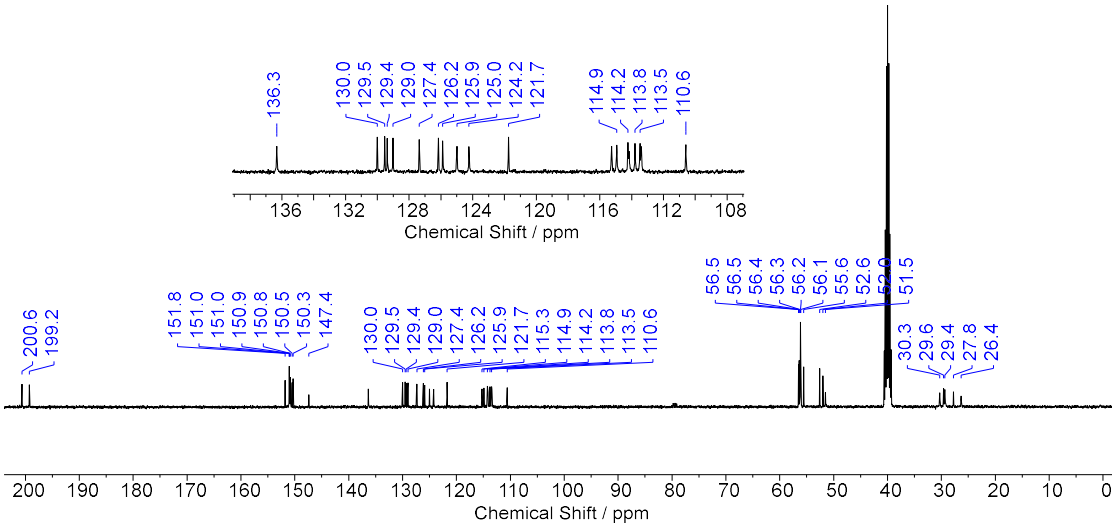

Fig. S13. (a) ^{1}H NMR (400 MHz) and (b) ^{13}C NMR (101 MHz) spectra of **MeP[5]DA-1** recorded in d_6-DMSO at 298 K.

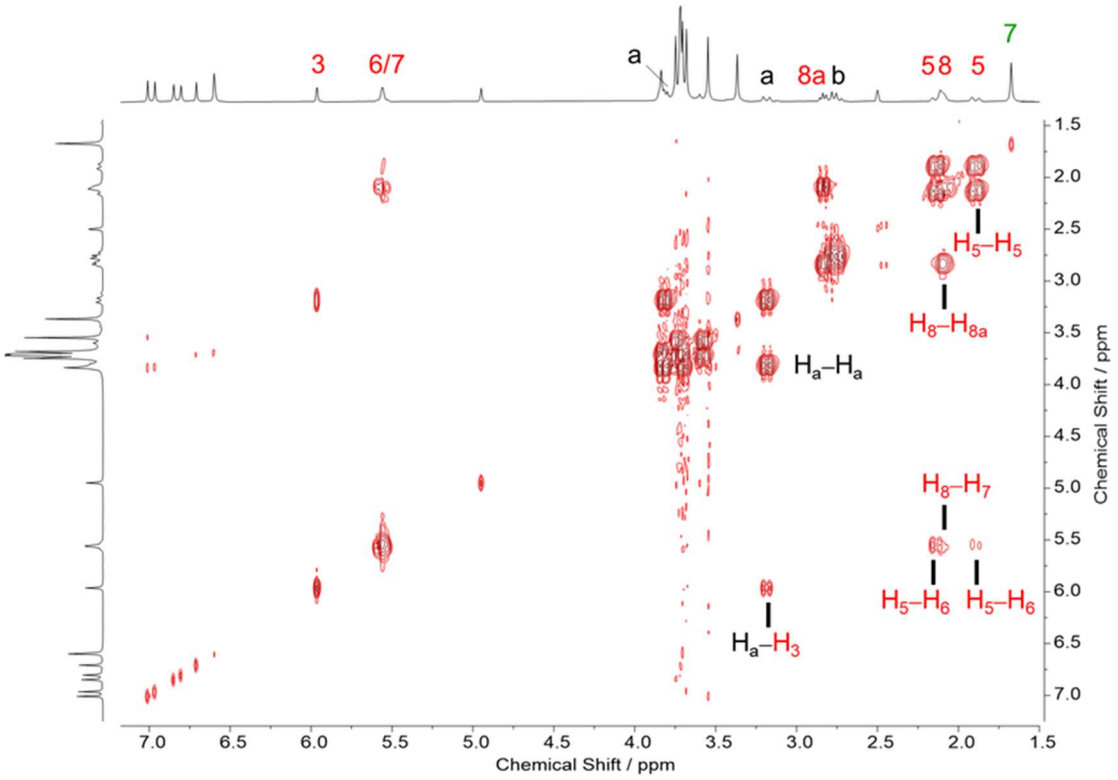

Fig. S14. ^{1}H–^{1}H COSY NMR spectrum of **MeP[5]DA-1** recorded in d_6-DMSO at 298 K.

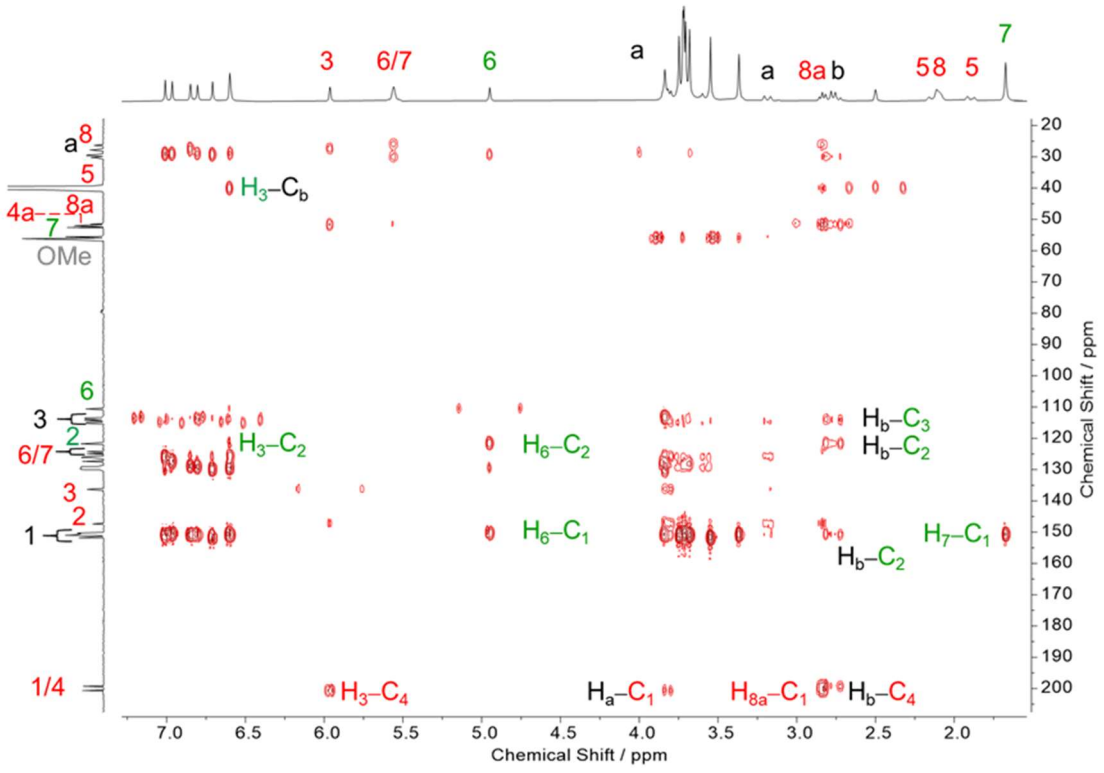

Fig. S15. ^{1}H–^{13}C HMBC NMR spectrum of **MeP[5]DA-1** recorded in d_6-DMSO at 298 K.

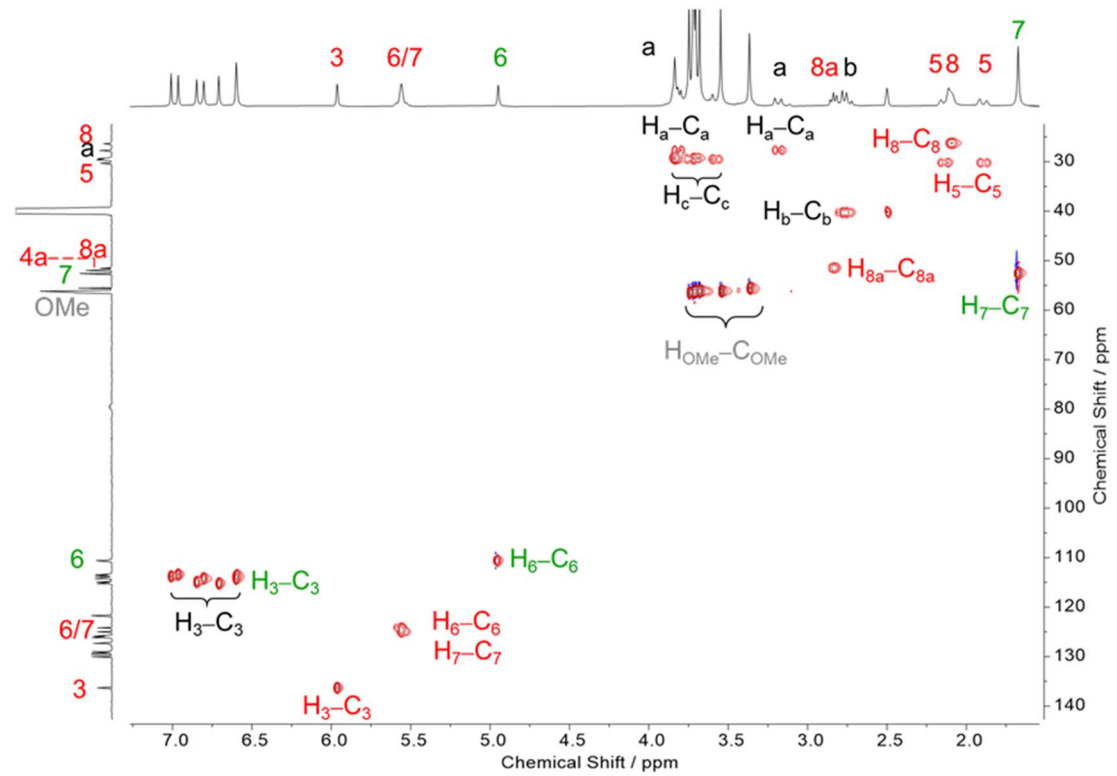

Fig. S16. ^{1}H–^{13}C HSQC NMR spectrum of **MeP[5]DA-1** recorded in d_6-DMSO at 298 K.

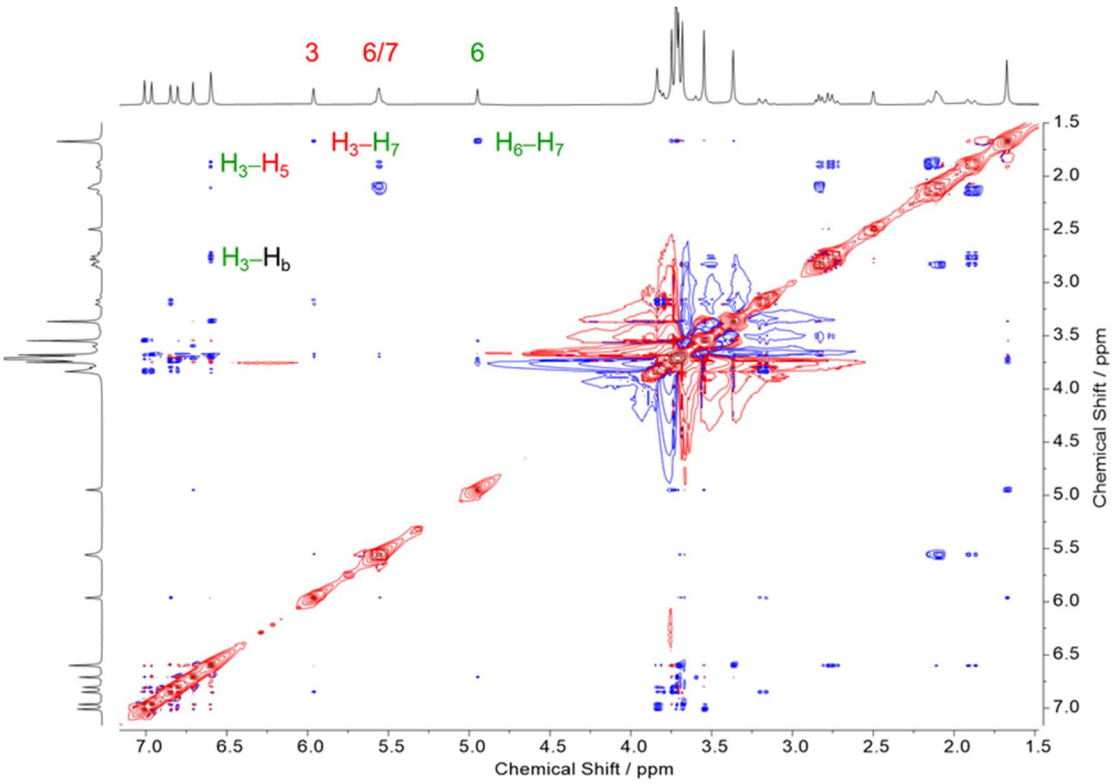

Fig. S17. ^{1}H–^{1}H ROESY NMR spectrum of **MeP[5]DA-1** recorded in d_6-DMSO at 298 K.

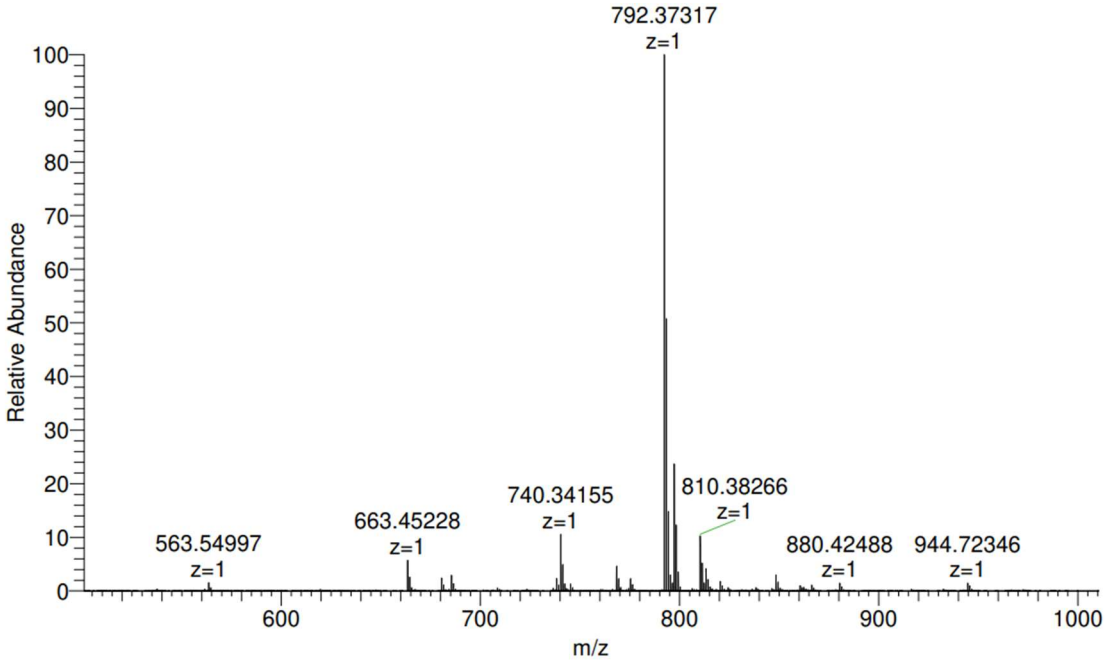

Fig. S18. Full ESI-MS spectrum of **MeP[5]DA-1** in positive mode.

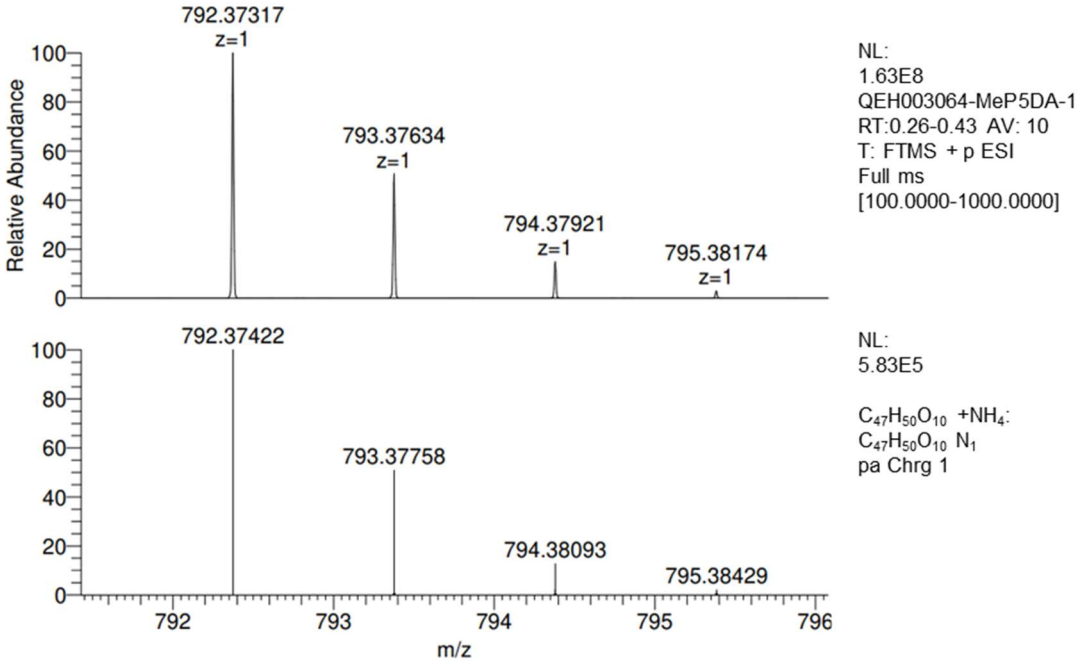

Fig. S19. Experimental (top) and stimulated (bottom) ESI-MS spectra of **MeP[5]DA-1**.

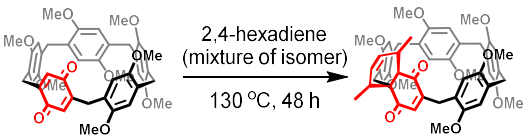

Scheme S2. Synthesis of **MeP[5]DA-2.**

MeP[5]DA-2: MeP[5]Q (400 mg, 0.56 mmol) and 2,4-hexadiene (mixture of isomer, 4 mL, 34 mmol) was added into a dried Schlenk vessel with teflon-protected vacuum valve. The mixture was heated at 130 °C and stirred for 24 h. Upon cooling to room temperature, the reaction mixture was concentrated under reduced pressure and purified by silica column chromatography (EtOAc/*n*-hexane, 1/3) and afford the product as yellow solid (98.4 mg, 22%). ^{1}H NMR (400 MHz, $CDCl_3$) δ 6.97 (s, 2H), 6.67 (s, 1H), 6.61 (s, 1H), 6.58 (s, 1H), 6.50 (s, 1H), 6.18 (d, J = 1.6 Hz, 1H), 5.61 (m, 2H), 5.52 (m, 1H), 4.02−3.91 (m, 3H), 3.86−3.58 (m, 26H), 3.05 (dd, J = 14.6, 1.9 Hz, 1H), 2.94 (s, 3H), 2.77 (d, J = 5.2 Hz, 1H), 2.58 (s, 3H), 2.52 (d, J = 15.2 Hz, 1H), 2.36 (m, 1H), 2.14 (m, 1H), 1.09 (d, J = 7.5 Hz, 1H), 0.79 (d, J = 7.3, 1H). ^{13}C NMR (101 MHz, $CDCl_3$) δ 202.6, 202.1, 155.6, 151.7, 151.6, 151.1, 151.0, 150.8, 150.6, 150.2, 135.1, 130.0, 129.8, 129.5, 129.4, 128.5, 126.9, 125.9, 125.4, 123.0, 114.6, 114.3, 114.2, 114.1, 114.1, 113.4, 111.2, 111.0, 56.2, 56.1, 56.1, 56.0, 56.0, 54.8, 54.1, 53.4, 49.8, 40.2, 39.8, 30.3, 30.1, 29.9, 29.0, 27.8, 19.0, 17.7. HRMS (ESI) *m/z* $[M + NH_4]^+$ Calcd for $C_{47}H_{54}O_{10}N$ 820.4055, found 820.4067

(a)

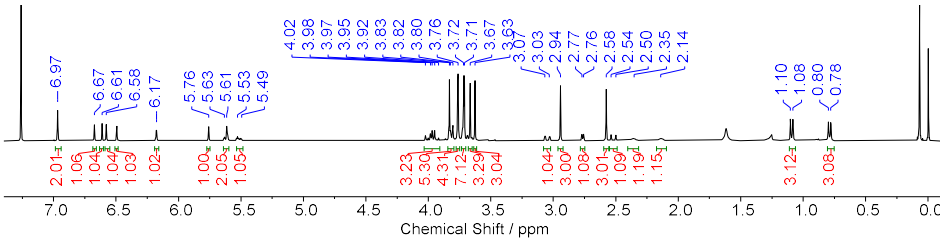

(b)

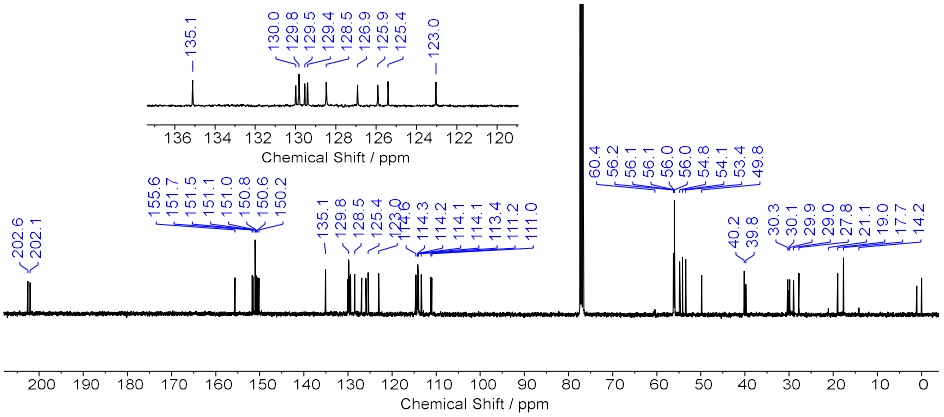

Fig. S20. (a) ^{1}H NMR (400 MHz) and (b) ^{13}C NMR (101 MHz) spectra of **MeP[5]DA-2** recorded in $CDCl_3$ at 298 K.

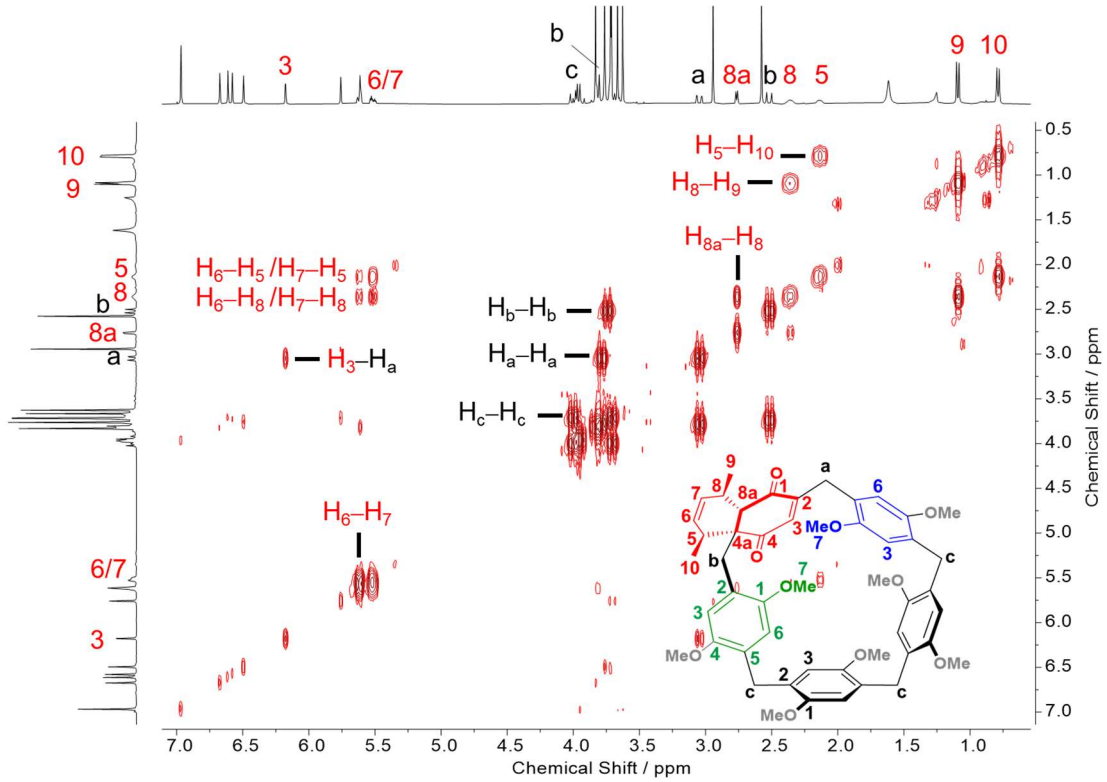

Fig. S21. ^{1}H–^{1}H COSY NMR spectra of **MeP[5]DA-2** recorded in $CDCl_3$ at 298 K.

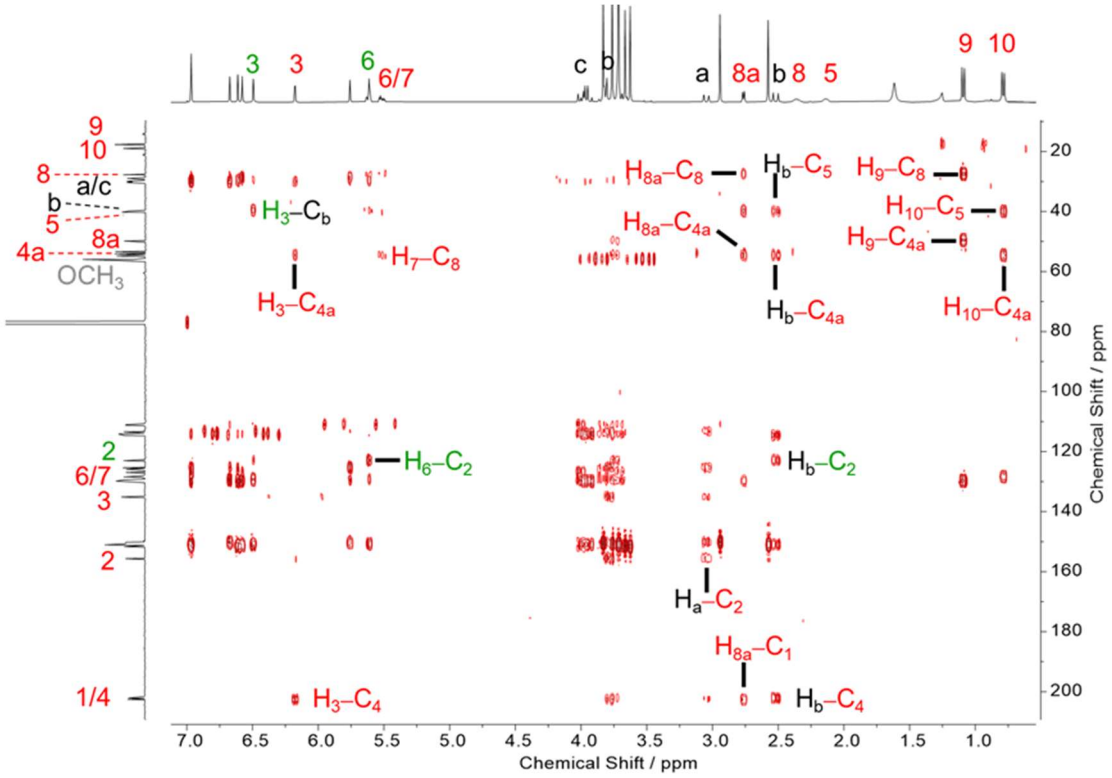

Fig. S22. ^{1}H–^{13}C HMBC NMR spectra of **MeP[5]DA-2** recorded in $CDCl_3$ at 298 K.

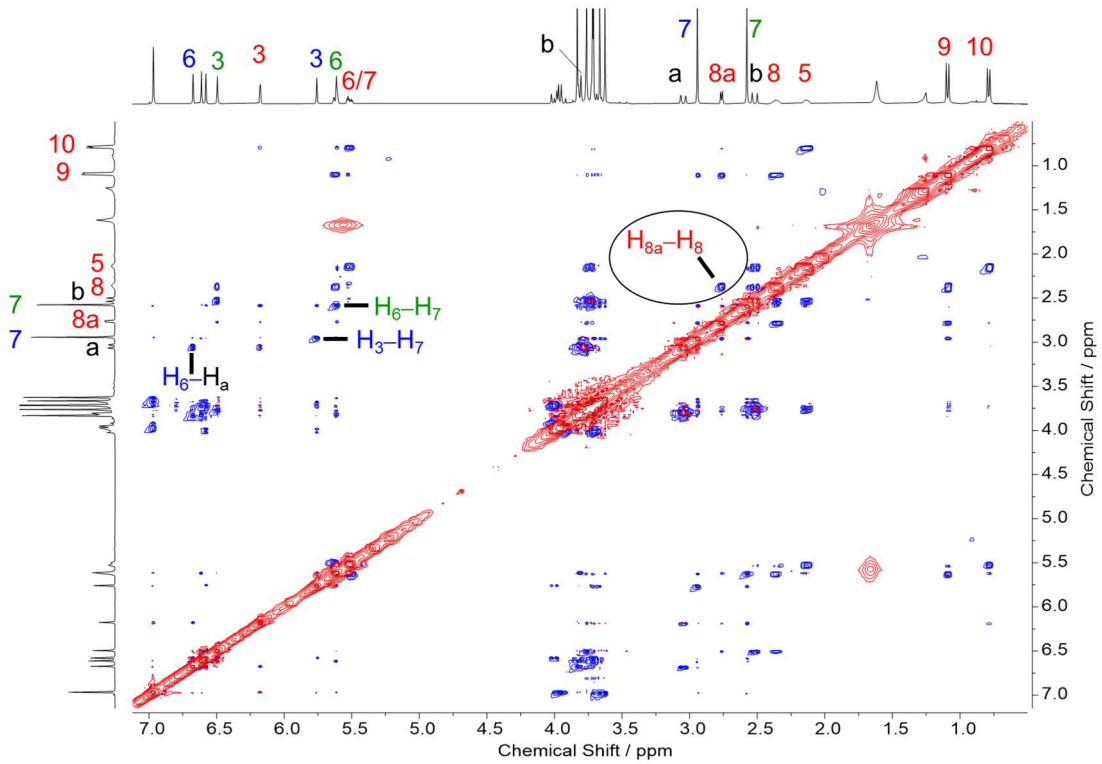

Fig. S23. $^{1}H–^{1}H$ NOESY NMR spectra of **MeP[5]DA-2** recorded in $CDCl_3$ at 298 K.

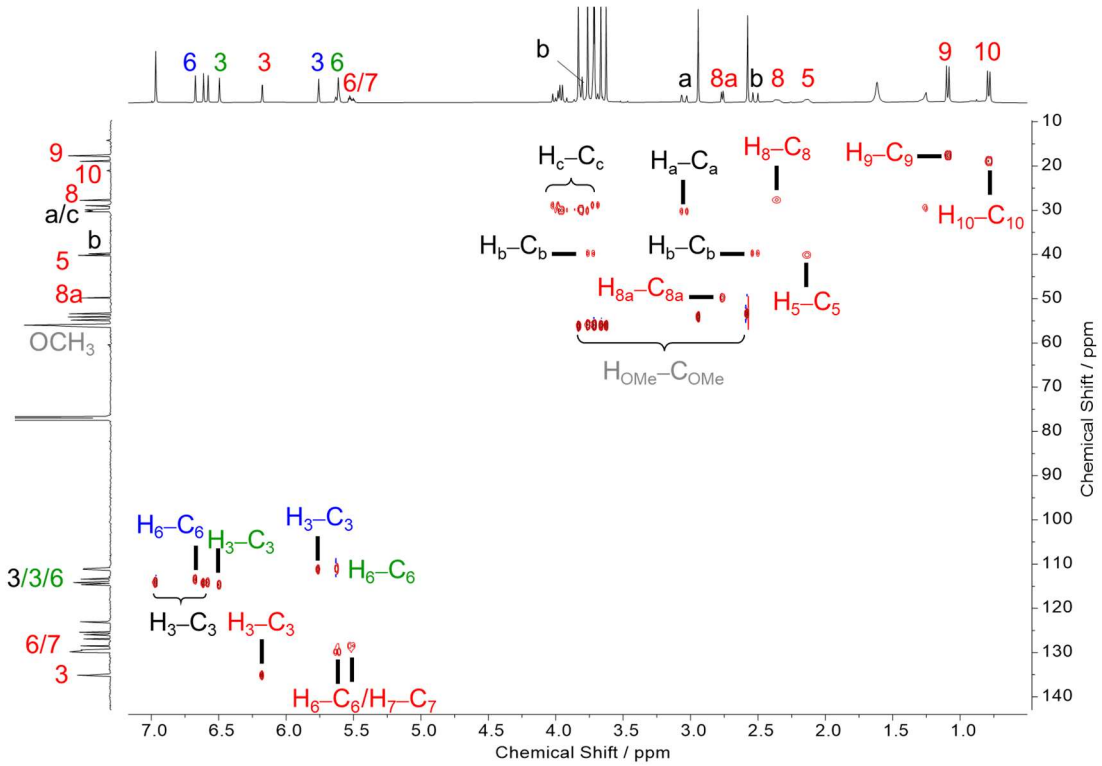

Fig. S24. $^{1}H–^{13}C$ HSQC NMR spectra of **MeP[5]DA-2** recorded in $CDCl_3$ at 298 K.

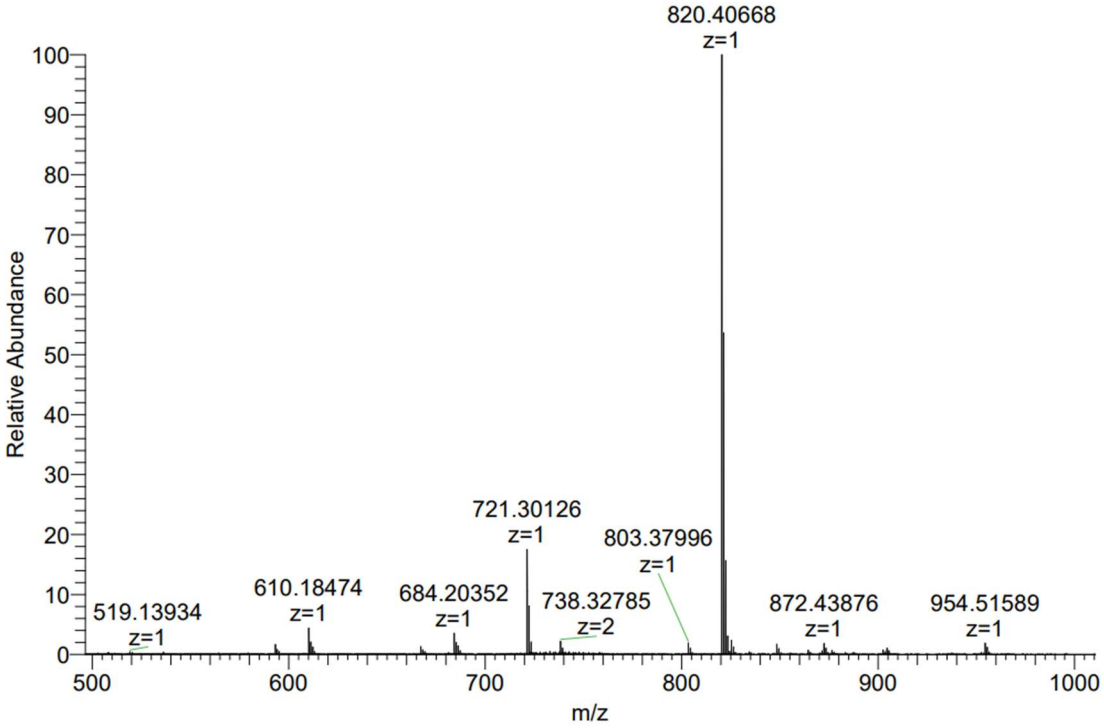

Fig. S25. Full ESI-MS spectrum of **MeP[5]DA-2** in positive mode.

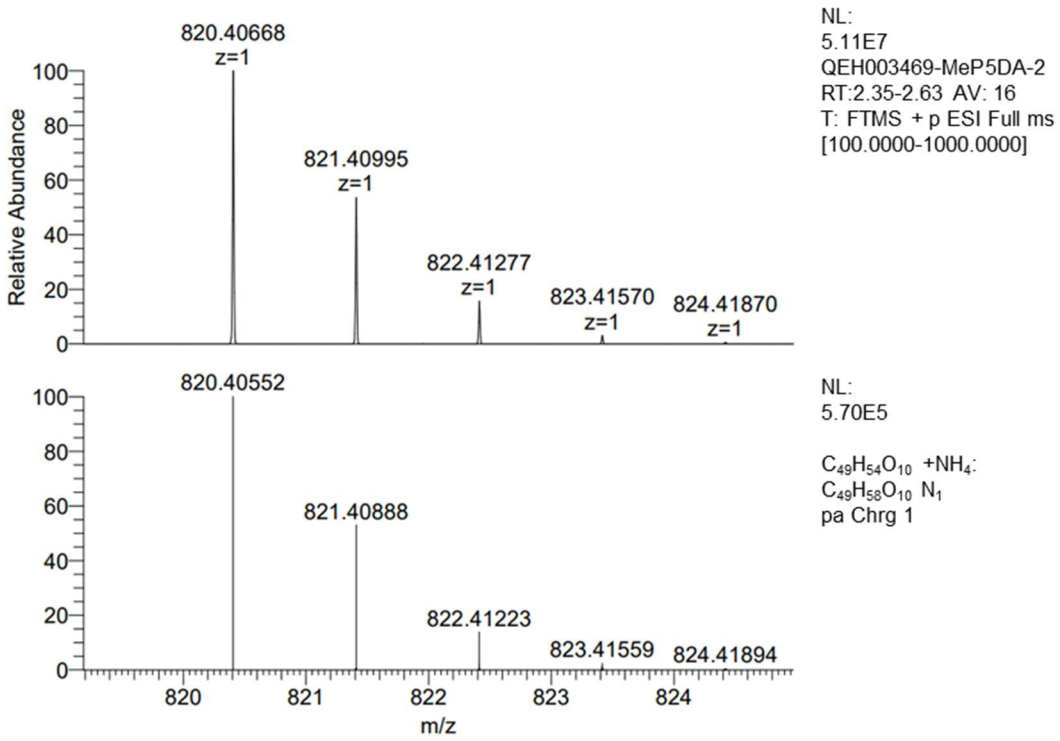

Fig. S26. Experimental (top) and stimulated (bottom) ESI-MS spectra of **MeP[5]DA-2**.

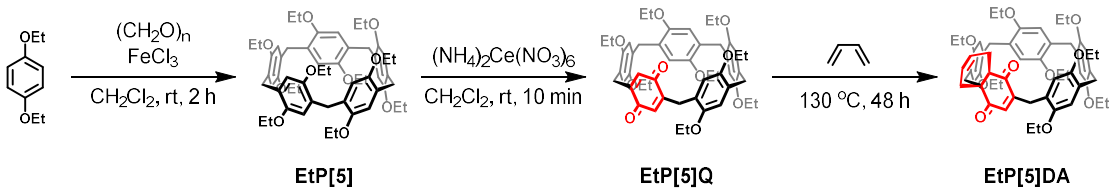

Scheme S3. Synthesis of **EtP[5]DA.**

EtP[5]: To a solution of 1,4-diethoxybenzene (1.66 g, 10 mmol) and $(CH_2O)_n$ (0.90 g, 30 mmol) in CH_2Cl_2 (150 mL), $FeCl_3$ (243 mg, 1.5 mmol) was added. The reaction mixture at 25 °C for 2 h. Water (200 mL) was poured into the reaction mixture. The organic phase was dried over Na_2SO_4 and concentrated under reduced pressure. The crude product was purified by silica column chromatography (CH_2Cl_2/*n*-hexane, 1/2) and afford the product as white solid (1.09 g, 61%). Data in accordance to literature.[4]

EtP[5]Q: To a solution of **EtP[5]** (890 mg, 1 mmol) in CH_2Cl_2 (100 mL) was added the solution of $(NH_4)_2Ce(NO_3)_6$ (1.1 g, 2 mmol) in water (5 mL) by dropwise, resulting in a red-coloured mixture which was stirred at 25 °C for 10 min. Water (100 mL) was added and the mixture was washed with copious amounts of water, the organic phase was dried over Na_2SO_4 and concentrated under reduced pressure. The residue was subjected to chromatography (EtOAc/*n*-hexane, 10/90) to afford the red solid product (340 mg, 41%). Data in accordance to literature.[5]

EtP[5]DA: EtP[5]Q (340 mg, 0.41 mmol) and 1,3-butadiene (1.9 mol/L in hexane, 10 mL, 19 mmol) was added into a dried Schlenk vessel with teflon-protected vacuum valve. The mixture was heated at 130 °C and stirred for 48 h. Upon cooling to room temperature, the reaction mixture was concentrated under reduced pressure and purified by silica column chromatography (EtOAc/*n*-hexane, 2/5) and afford the product as yellow solid (165 mg, 45%). ^{1}H NMR (400 MHz, $CDCl_3$) δ 6.98 (s, 1H), 6.92 (s, 1H), 6.76 (s, 1H), 6.64 (s, 1H), 6.60 (s, 2H), 6.48 (s, 1H), 6.45 (s, 1H), 5.89 (s, 1H), 5.72 (d, J = 10.0 Hz, 1H), 5.57 (d, J = 9.8 Hz, 1H), 4.03–3.59 (m, 20H), 3.34 (d, J = 14.7 Hz, 1H), 3.17 (d, J = 14.2 Hz, 1H), 2.99 (d, J = 6.9 Hz, 2H), 2.89 (d, J = 14.2 Hz, 1H), 2.79 (d, J = 6.2, 4.1 Hz, 1H), 2.39 (d, J = 18.2 Hz, 1H), 2.32–2.23 (m, 1H), 2.16–2.05 (m, 1H), 1.87 (d, J = 18.9 Hz, 1H), 1.49–1.34 (m, 12H), 1.31–1.21 (m, 6H), 1.10 (t, J = 6.9 Hz, 3H), 0.48 (t, J = 6.9 Hz, 3H). ^{13}C NMR (101 MHz, $CDCl_3$) δ 200.8, 199.9, 149.6, 149.4, 149.2, 148.9, 148.9, 148.8, 148.8, 148.6, 147.9, 135.0, 128.9, 128.8, 128.5, 128.4, 127.0, 126.1, 124.2, 122.6, 122.2, 122.1, 114.9, 114.5, 114.3, 114.0, 113.9, 113.7, 113.2, 112.7, 63.5, 63.3, 63.2, 63.0, 62.9, 62.8, 62.3, 61.4, 50.9, 48.1, 32.2, 29.1, 28.8, 28.1, 21.7, 14.3, 14.3, 14.2, 14.2, 14.0, 13.9, 13.7, 12.4. HRMS (ESI) *m/z* $[M + NH_4]^+$ Calcd for $C_{47}H_{54}O_{10}N$ 904.4994, found 904.5010.

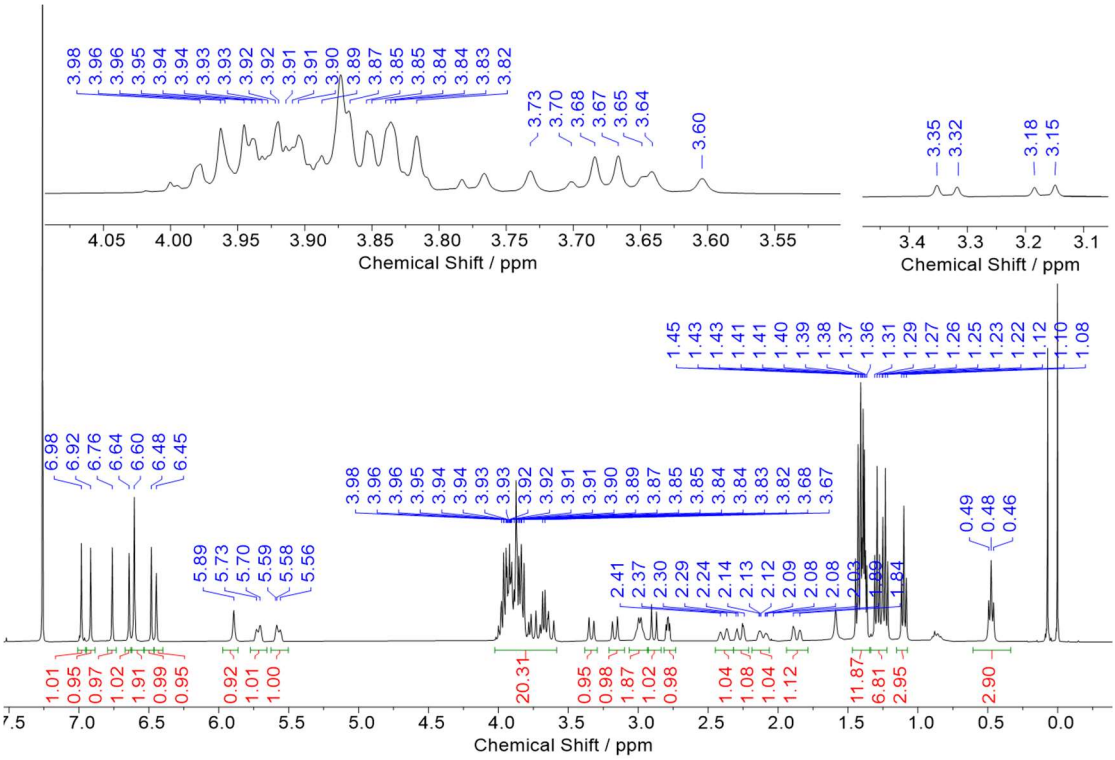

Fig. S27. ^{1}H NMR (400 MHz) spectrum of **EtP[5]DA** recorded in $CDCl_3$ at 298 K.

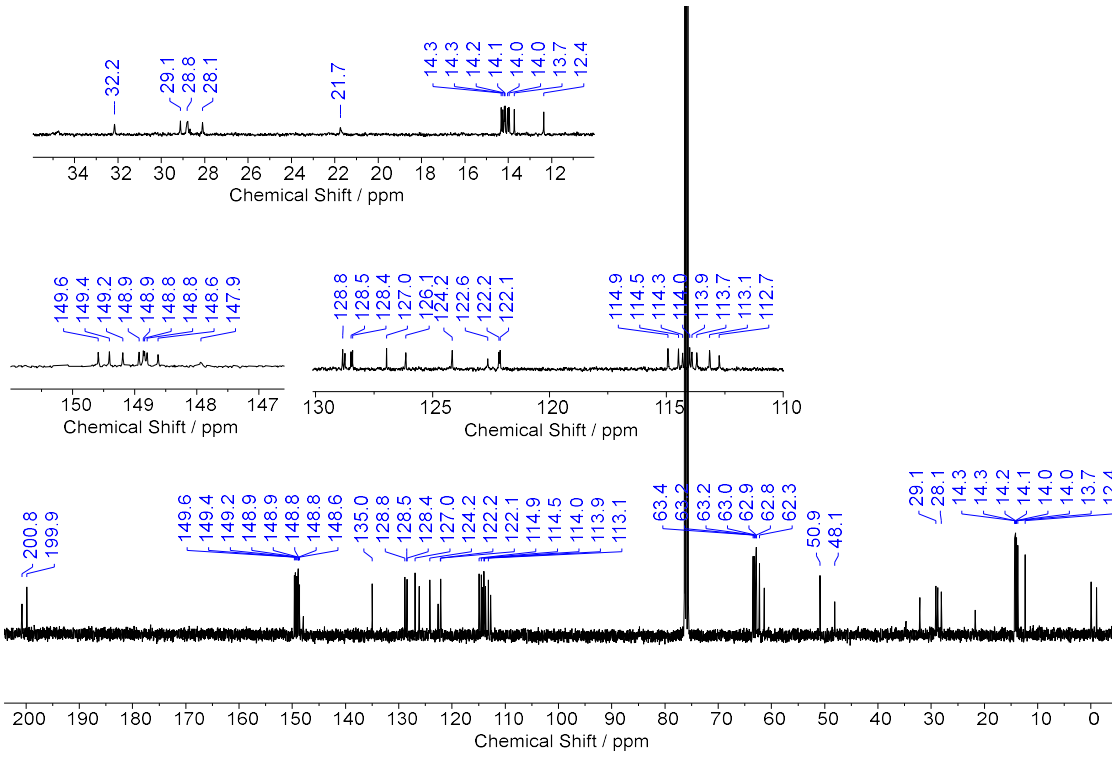

Fig. S28. ^{1}H NMR (400 MHz) spectrum of **EtP[5]DA** recorded in $CDCl_3$ at 298 K.

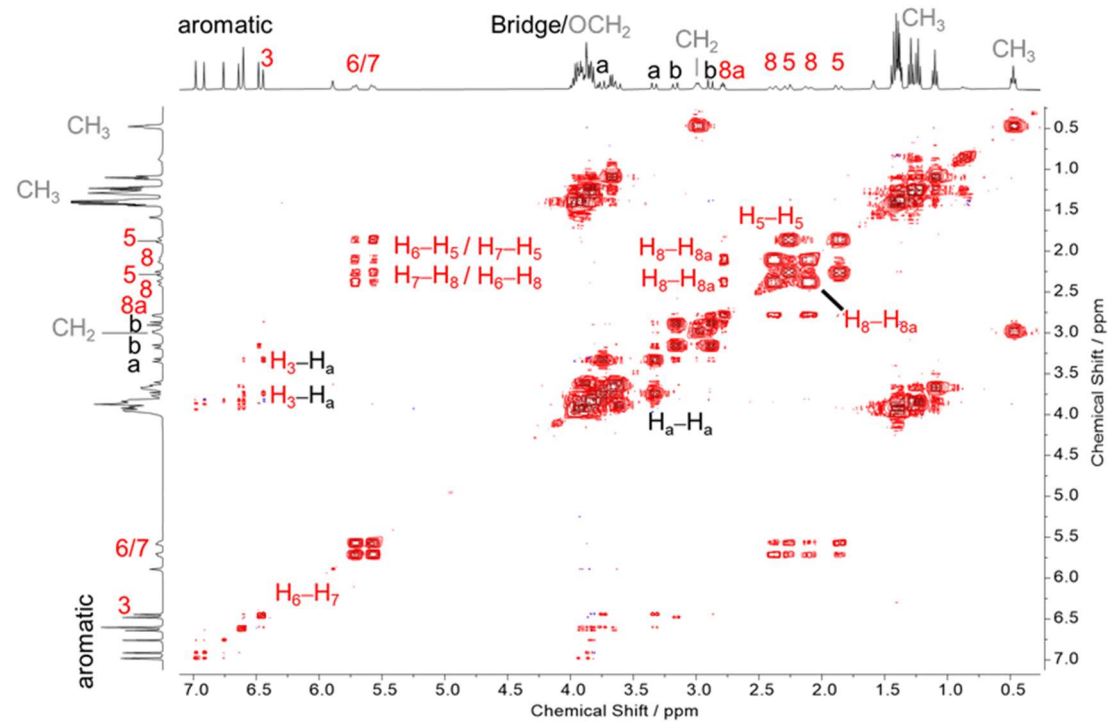

Fig. S29. $^{1}H–^{1}H$ COSY NMR spectra of **EtP[5]DA** recorded in $CDCl_3$ at 298 K.

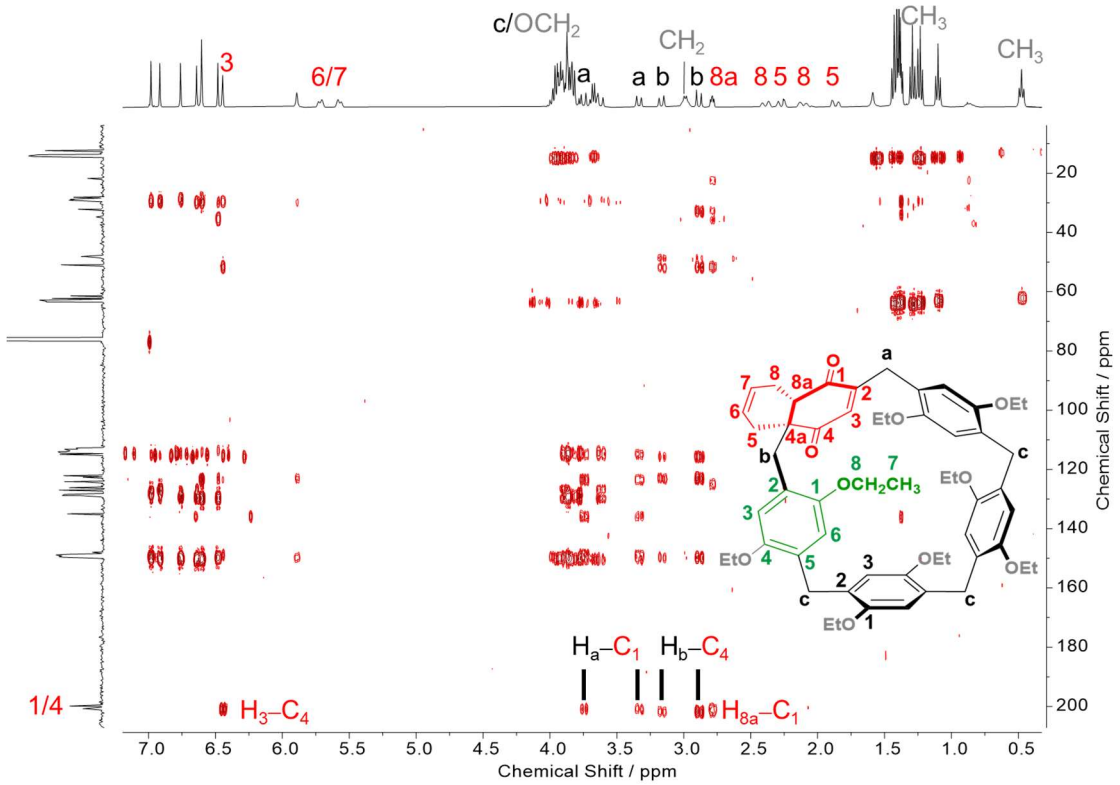

Fig. S30. $^{1}H–^{13}C$ HMBC NMR spectra of **EtP[5]DA** recorded in $CDCl_3$ at 298 K.

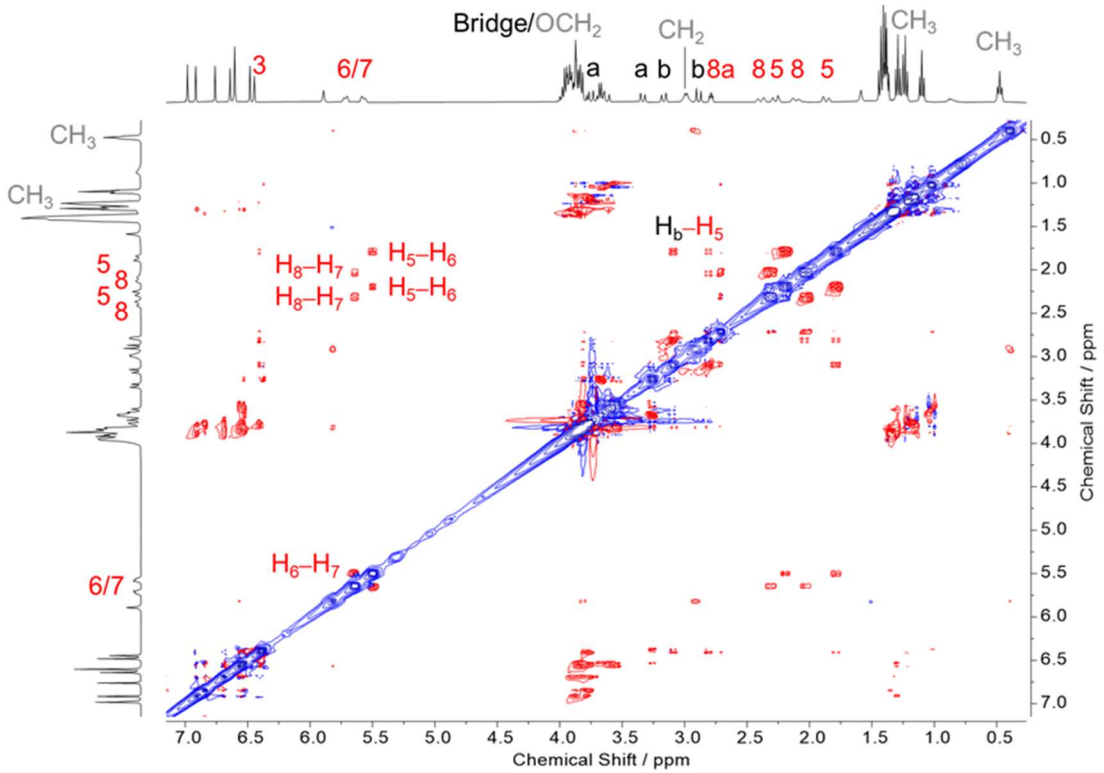

Fig. S31. ^{1}H–^{1}H ROESY NMR spectra of **EtP[5]DA** recorded in $CDCl_3$ at 298 K.

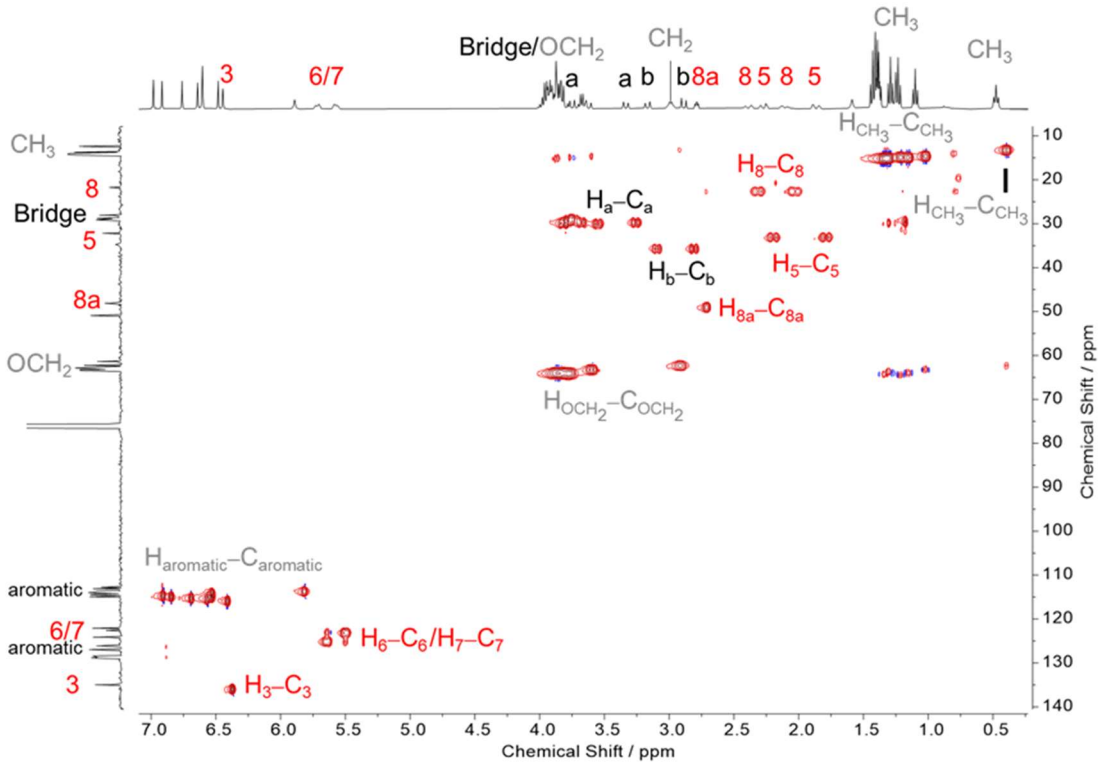

Fig. S32. ^{1}H–^{13}C HSQC NMR spectra of **EtP[5]DA** recorded in $CDCl_3$ at 298 K.

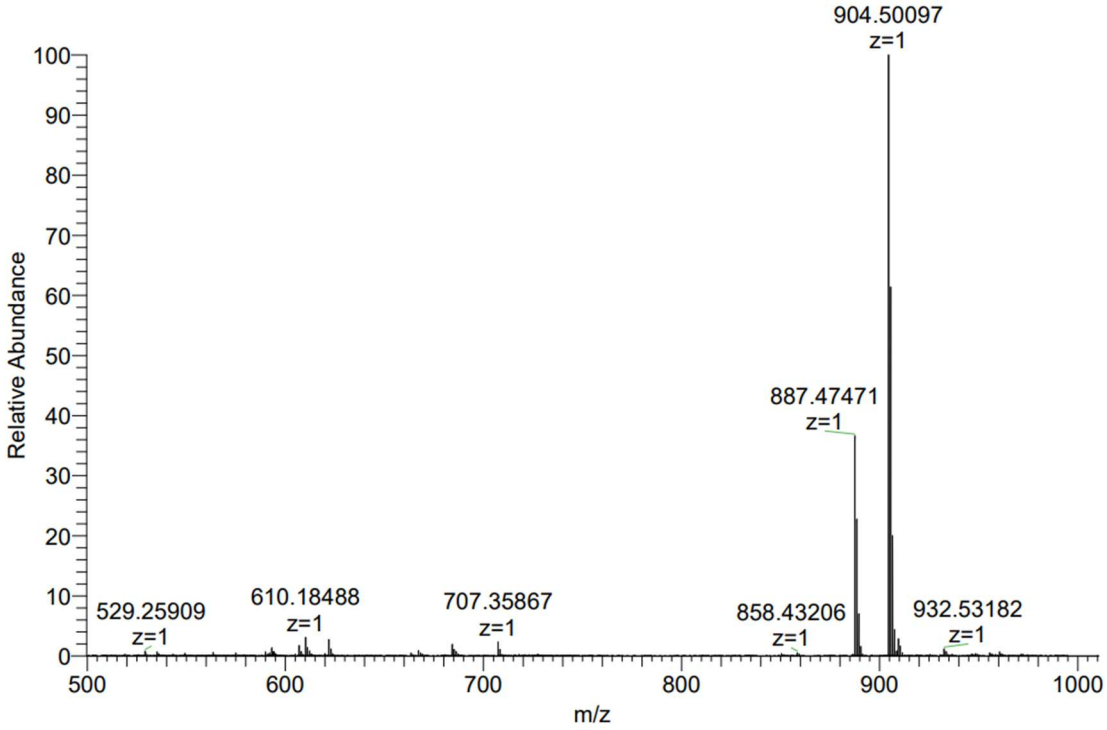

Fig. S33. Full ESI-MS spectrum of **EtP[5]DA** in positive mode.

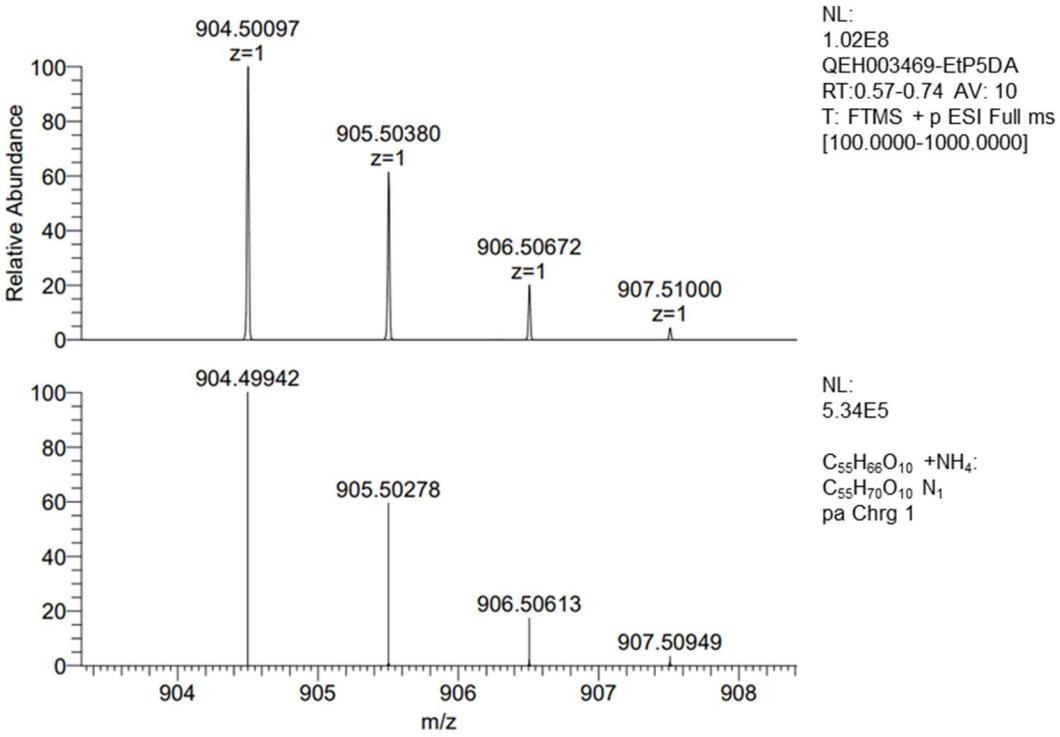

Fig. S34. Experimental (top) and stimulated (bottom) ESI-MS spectra of **EtP[5]DA**.

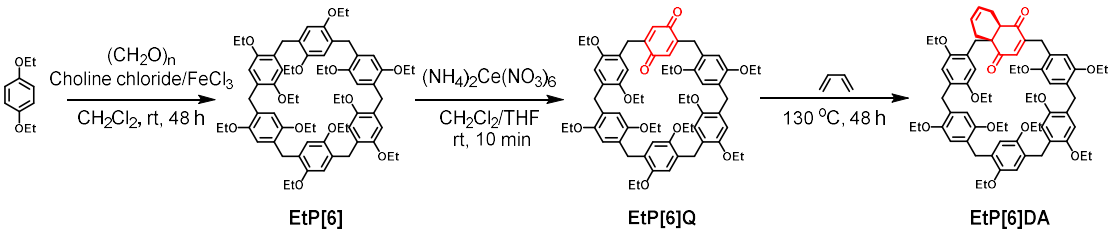

Scheme S4. Synthesis of **EtP[6]DA.**

EtP[6]: The mixture of choline chloride (2.5 g, 18 mmol) and $FeCl_3$ (5.8 g, 36 mmol) was heated until dark solution formed. To a solution of 1,4-diethoxybenzene (19.9 g, 120 mmol) and $(CH_2O)_n$ (10.8 g, 360 mmol) in CH_2Cl_2 (1800 mL) was added the solution. The reaction mixture was stirred at 25 °C for 48 h and quenched by addition of water. The organic phase was washed with saturated aqueous $NaHCO_3$. The crude product was purified by silica column chromatography (EtOAc/*n*-hexane, 1/15) and afford the product as white solid (7.98 g, 37%). Data in accordance to literature.[6]

EtP[6]Q: A solution of $(NH_4)_2Ce(NO_3)_6$ (0.56 g, 1.03 mmol, dissolved in 10 mL water) was added dropwise into the solution of **EtP[6]** (500 mg, 0.47 mmol) in 50 mL of CH_2Cl_2/THF (1:1) and the reaction mixture was stirred at room temperature for 20 h. The mixture was washed with copious amounts of water, the organic phase was dried and concentrated. The residue was subjected to chromatography (EtOAc/*n*-hexane, 10/90) to obtain **EtP[6]Q** (0.24 g, 50%). Data in accordance to literature.[7]

EtP[6]DA: EtP[6]Q (101 mg, 0.1 mmol) and 1,3-butadiene (1.9 mol/L in hexane, 3.5 mL, 6.7 mmol) was added into a dried Schlenk vessel with teflon-protected vacuum valve. The mixture was heated at 130 °C and stirred for 48 h. Upon cooling to room temperature, the reaction mixture was concentrated under reduced pressure and purified by silica column chromatography (EtOAc/*n*-hexane, 2/5) and afford the product as yellow solid (26.6 mg, 25%). ^{1}H NMR (400 MHz, $CDCl_3$) δ 6.88 (s, 1H), 6.82 (s, 1H), 6.78 (s, 1H), 6.74 (s, 1H), 6.69 (s, 1H), 6.65 (s, 1H), 6.57 (s, 1H), 6.53 (s, 1H), 6.06 (s, 1H), 5.78−5.79 (m, 1H), 5.57−5.61 (m, 2H), 3.66−3.97 (m, 24H), 3.30−3.34 (dd, J = 17.2, 2.0 Hz, 1H), 3.20−3.28 (m, 2H), 3.14 (d, J = 13.2 Hz, 1H), 2.96 (t, J = 6.4 Hz, 1H), 2.73 (d, J = 13.2 Hz, 1H), 1.10−1.37 (m, 27H), 0.529 (t, J = 7.2 Hz, 3H). ^{13}C NMR (100 MHz, $CDCl_3$) δ 202.1, 200.6, 150.8, 150.8, 150.7, 150.7, 150.5, 150.5, 150.5, 150.0, 147.8, 135.5, 130.4, 130.1, 129.7, 129.0, 125.51, 128.6, 128.5, 128.2, 127.4, 124.9, 123.9, 123.0, 122.4, 116.3, 116.2, 115.5, 115.3, 115.2, 115.1, 114.9, 113.9, 64.8, 64.6, 64.4, 64.3, 64.3, 64.2, 64.1, 64.0, 63.9, 63.8, 60.5, 53.2, 52.8, 40.2, 32.9, 30.8, 30.7, 30.6, 30.5, 30.2, 29.8, 26.5, 21.2, 15.4, 15.3, 15.3, 15.3, 15.2, 15.1, 15.1, 14.3, 14.2. HRMS (ESI) *m/z* $[M + NH_4]^+$ Calcd for $C_{66}H_{84}O_{12}N$ 1082.5988, found 1082.5981.

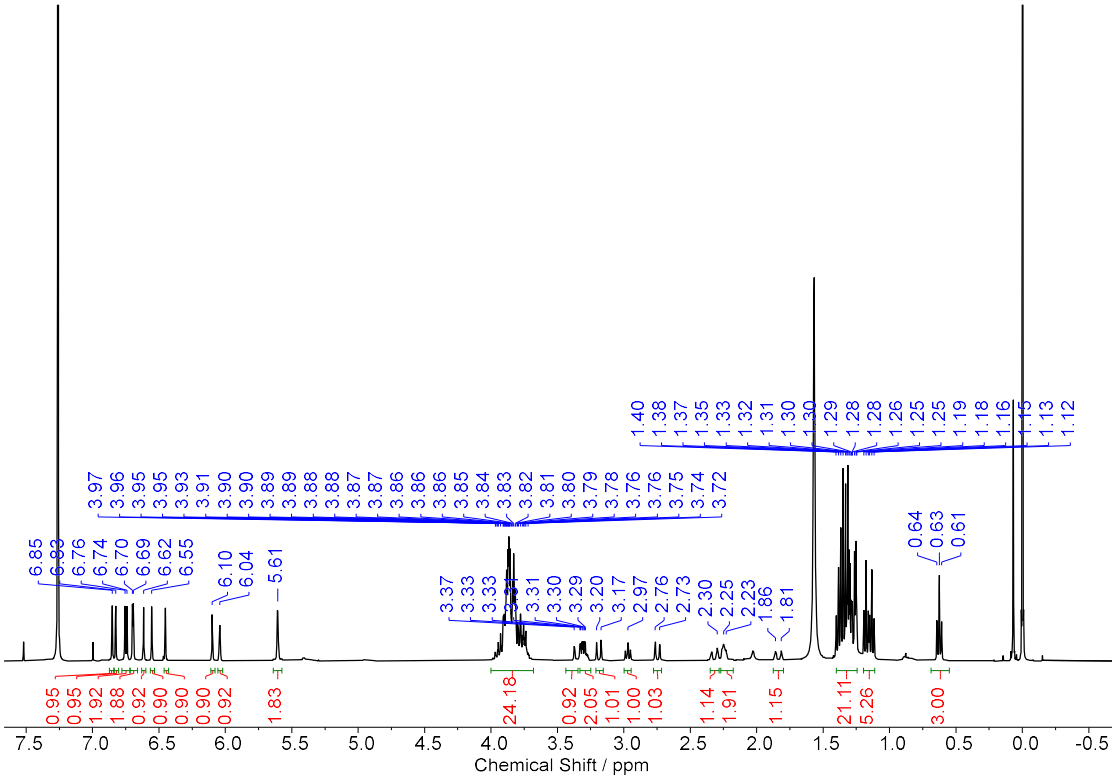

Fig. S35. ^{1}H NMR (400 MHz) spectrum of **EtP[6]DA** recorded in $CDCl_3$ at 298 K.

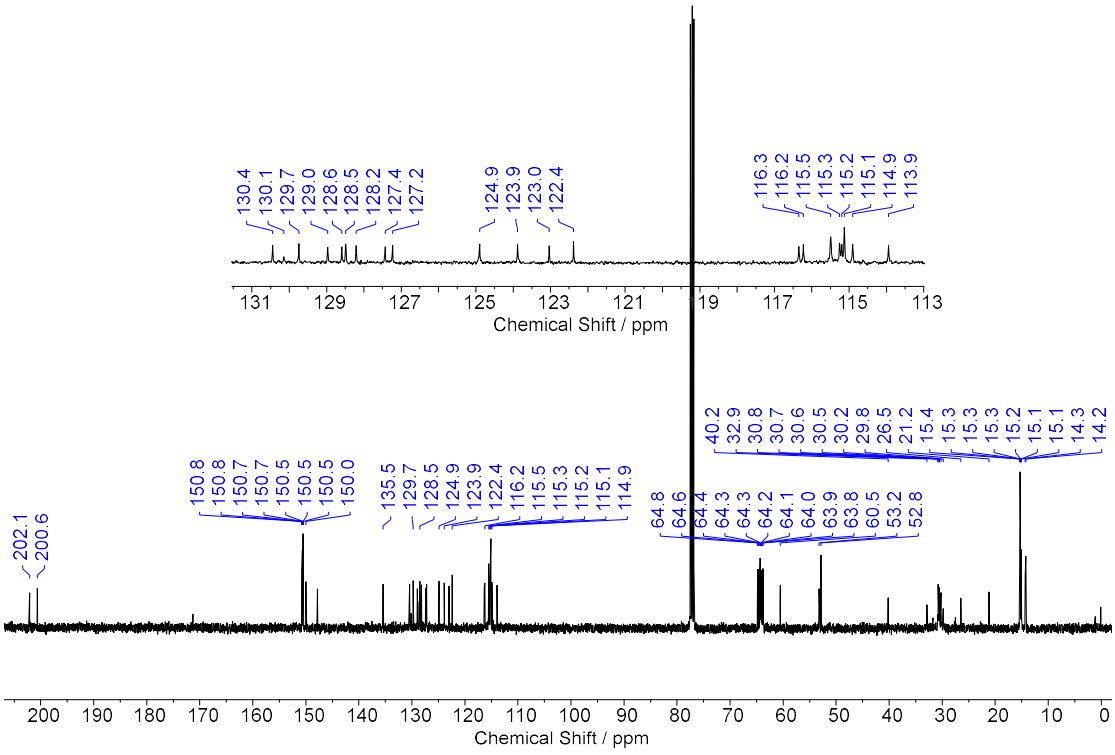

Fig. S36. ^{13}C NMR (100 MHz) spectrum of **EtP[6]DA** recorded in $CDCl_3$ at 298 K.

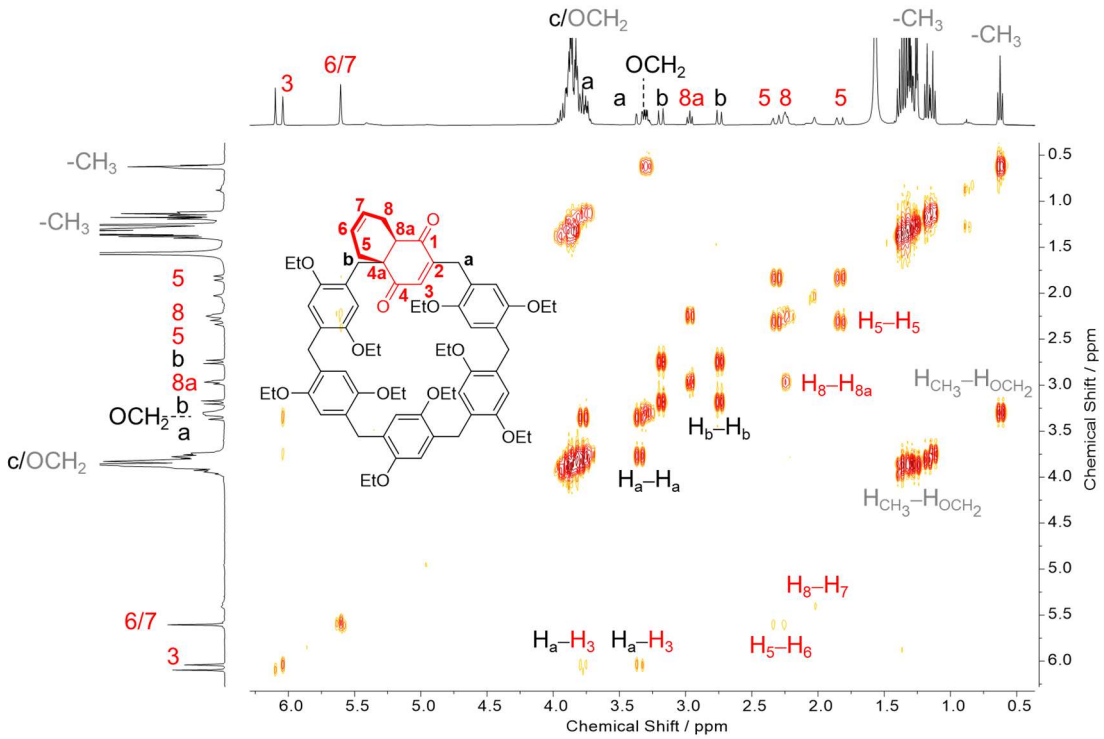

Fig. S37. ^{1}H–^{1}H COSY NMR spectrum (400 MHz) of **EtP[6]DA** recorded in $CDCl_3$ at 298 K.

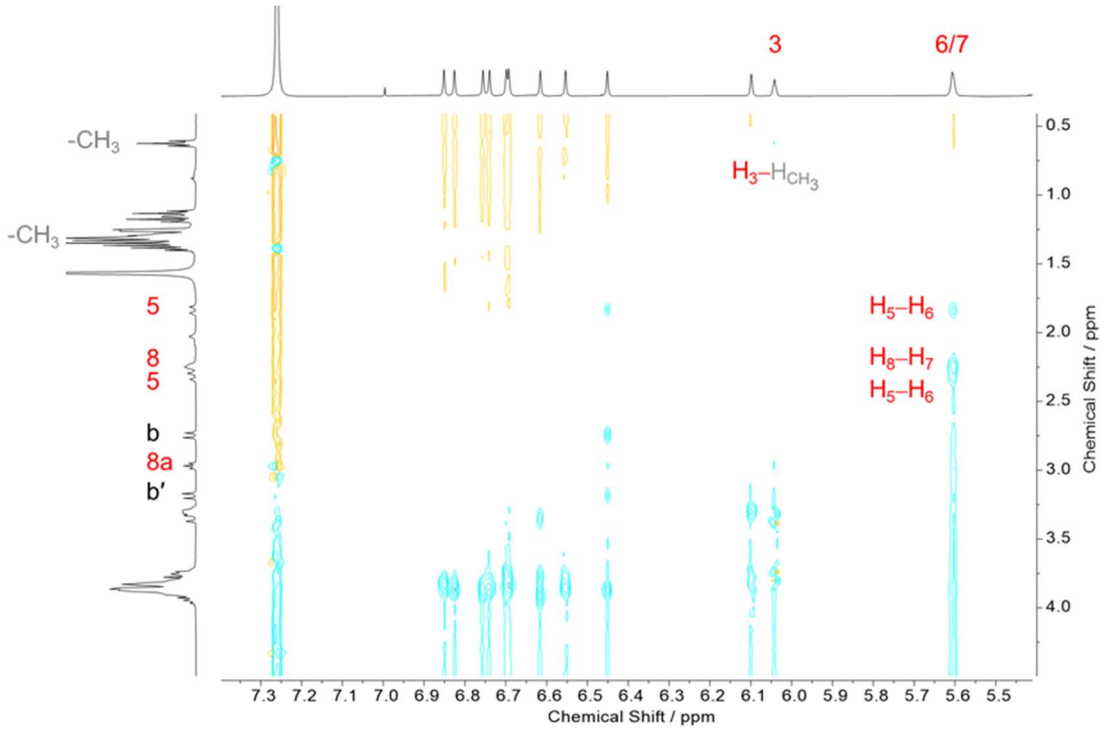

Fig. S38. ^{1}H–^{1}H ROESY NMR spectrum (400 MHz) of **EtP[6]DA** recorded in $CDCl_3$ at 298 K.

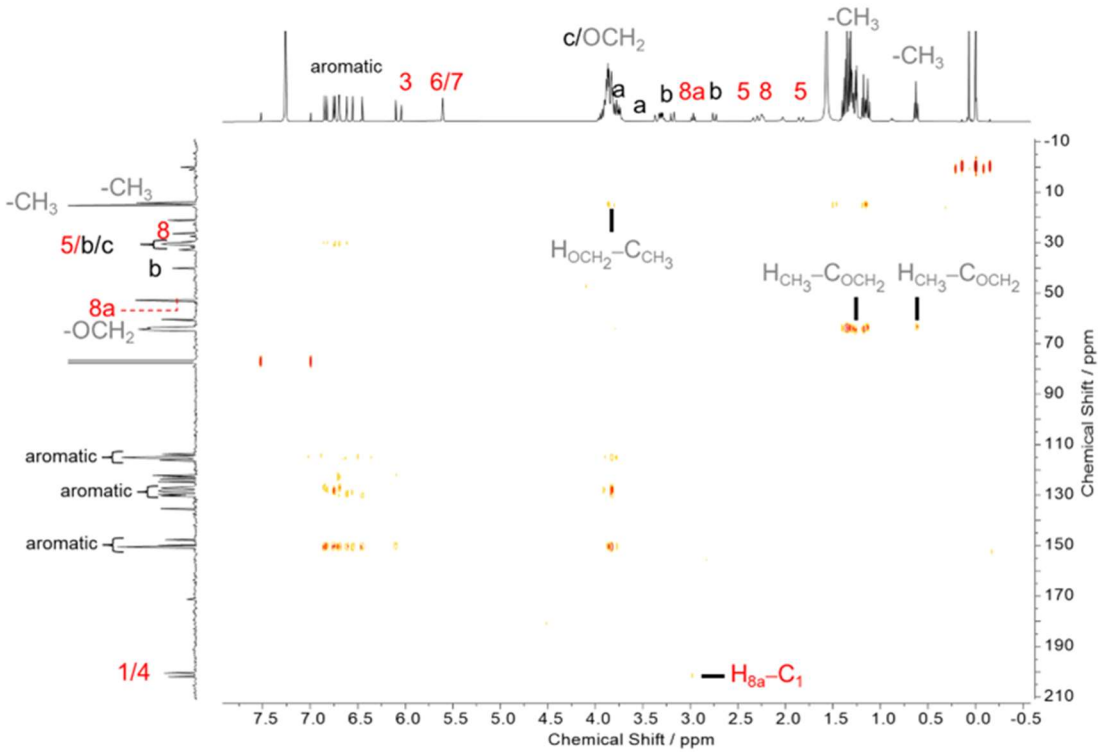

Fig. S39. $^{1}H–^{13}C$ HMBC NMR spectrum of **EtP[6]DA** recorded in $CDCl_3$ at 298 K.

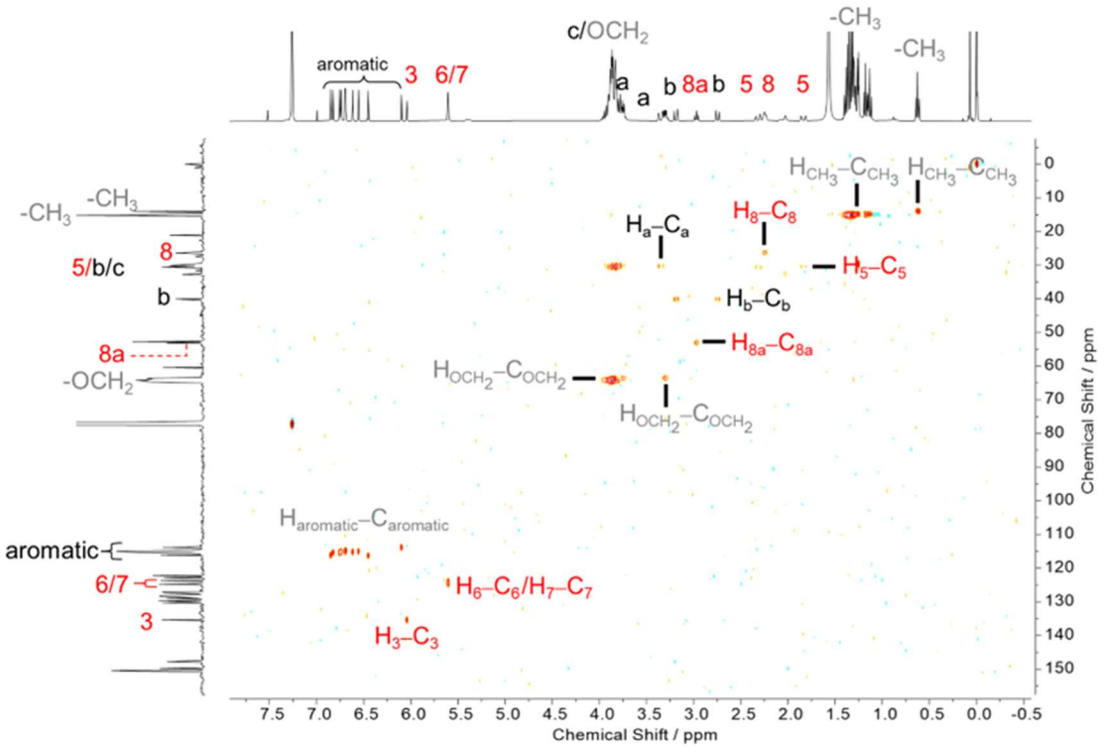

Fig. S40. $^{1}H–^{13}C$ HSQC NMR spectrum of **EtP[6]DA** recorded in $CDCl_3$ at 298 K.

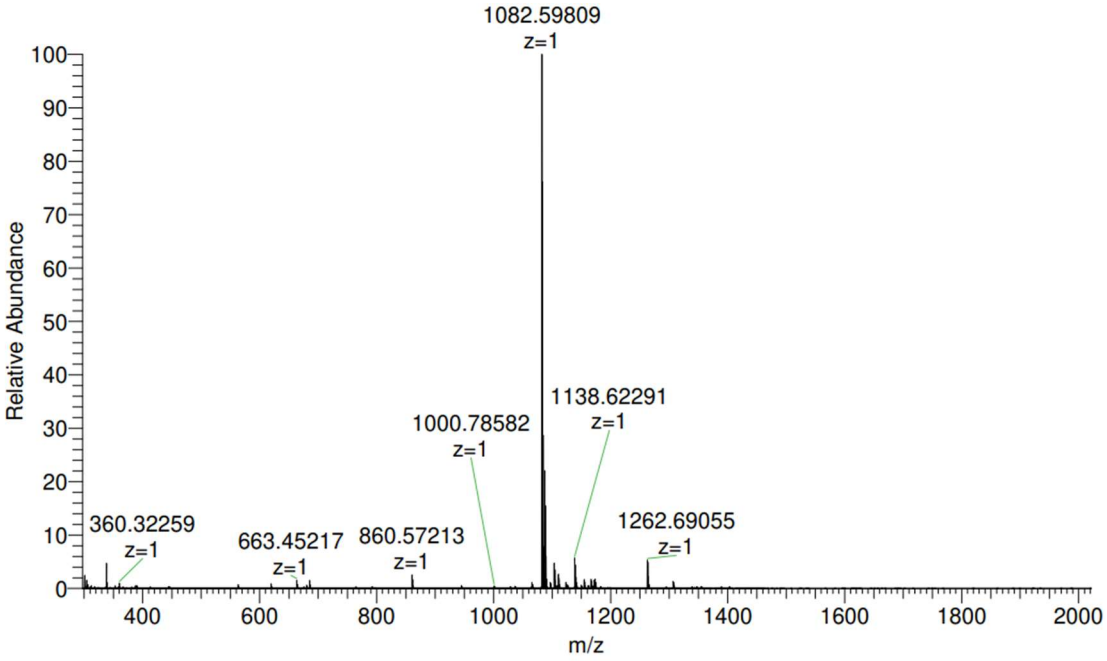

Fig. S41. Full ESI-MS spectrum of **EtP[6]DA** in positive mode.

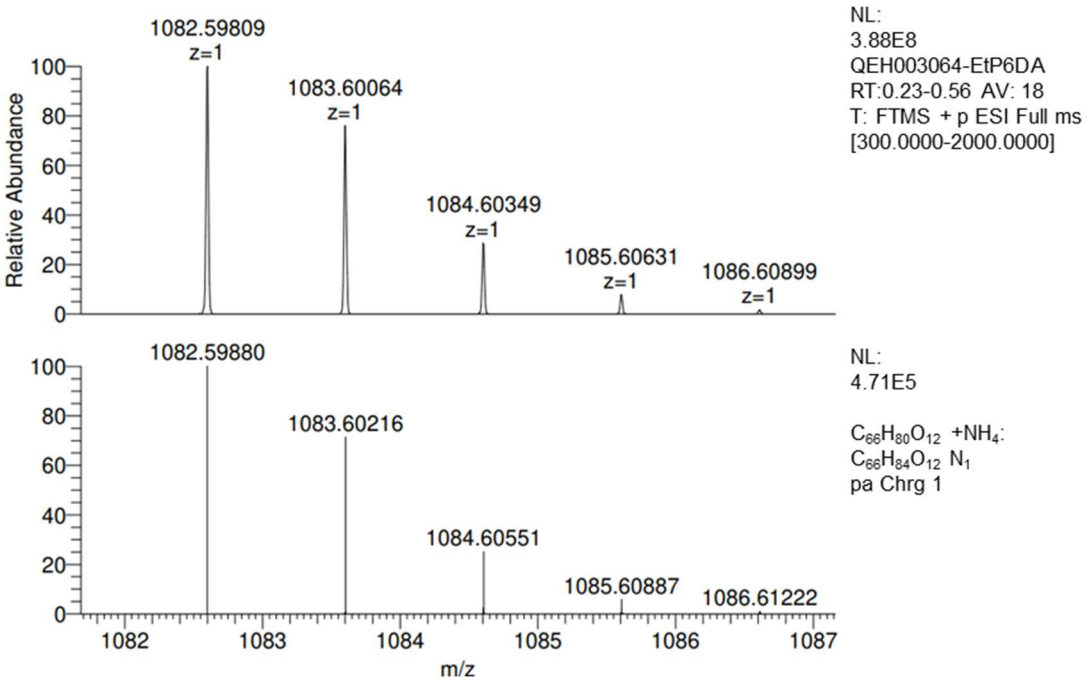

Fig. S42. Experimental (top) and stimulated (bottom) ESI-MS spectra of **EtP[6]DA**.

3. Conformational Change Studies

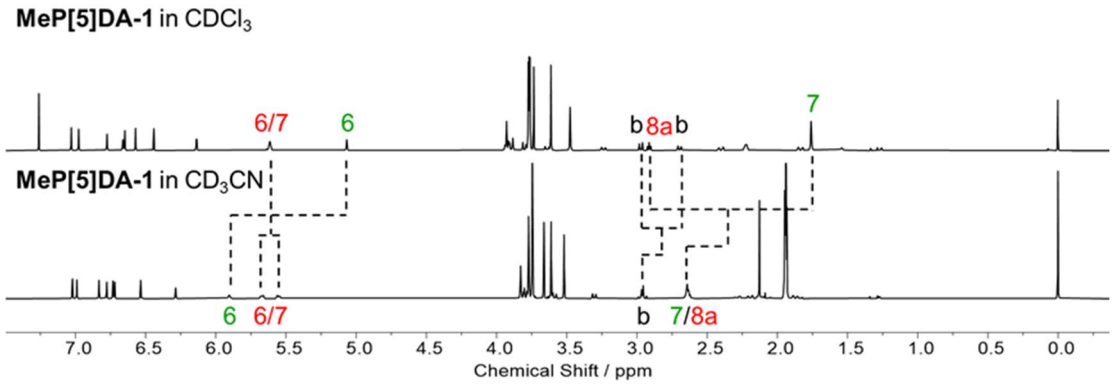

Fig. S43. ^{1}H NMR spectra of **MeP[5]DA-1** recorded in $CDCl_3$ and CD_3CN at 298 K.

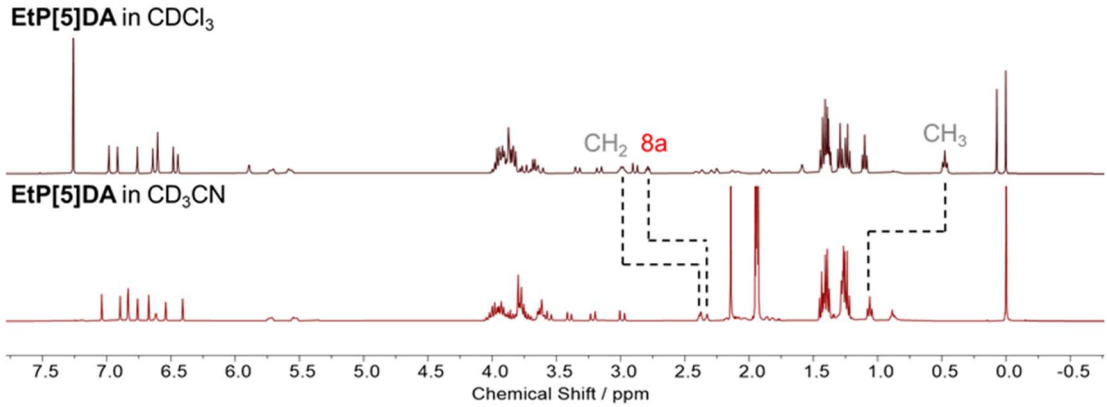

Fig. S44. ^{1}H NMR spectra of **EtP[5]DA** recorded in $CDCl_3$ and CD_3CN at 298 K.

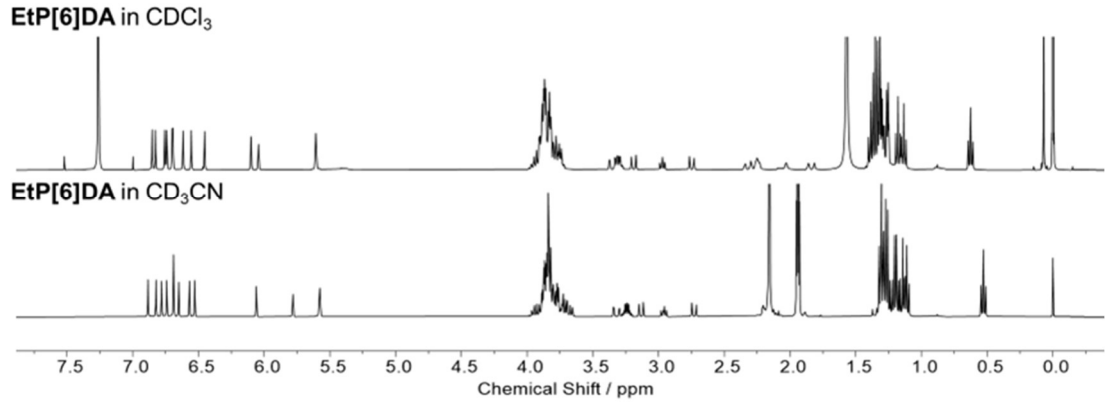

Fig. S45. Overlaid ^{1}H NMR spectra of **EtP[6]DA** recorded in $CDCl_3$ (top) and CD_3CN (bottom) at 298 K.

4. X-Ray Crystallography

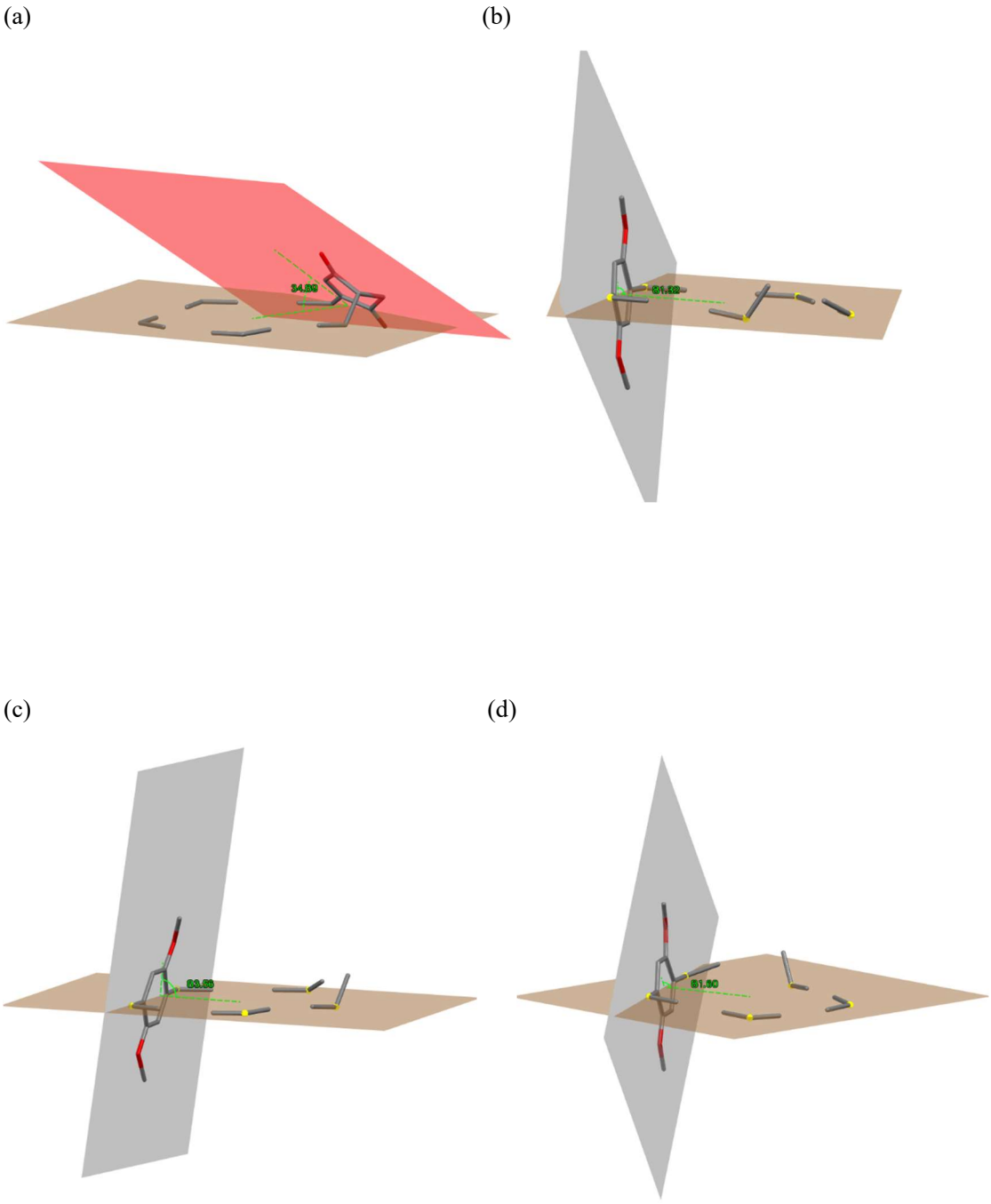

Fig. S46. Partial crystal Structures of **MeP[5]DA-1**. (a) 1,4-dione ring A (red), (b) Ring C (grey), (c) Ring D (grey) and (d) Ring E (grey) form a dihedral angle of 34.89°/81.32°/83.56°/81.60° with the bridge methylene plane (brown). The yellow atoms are methylene.

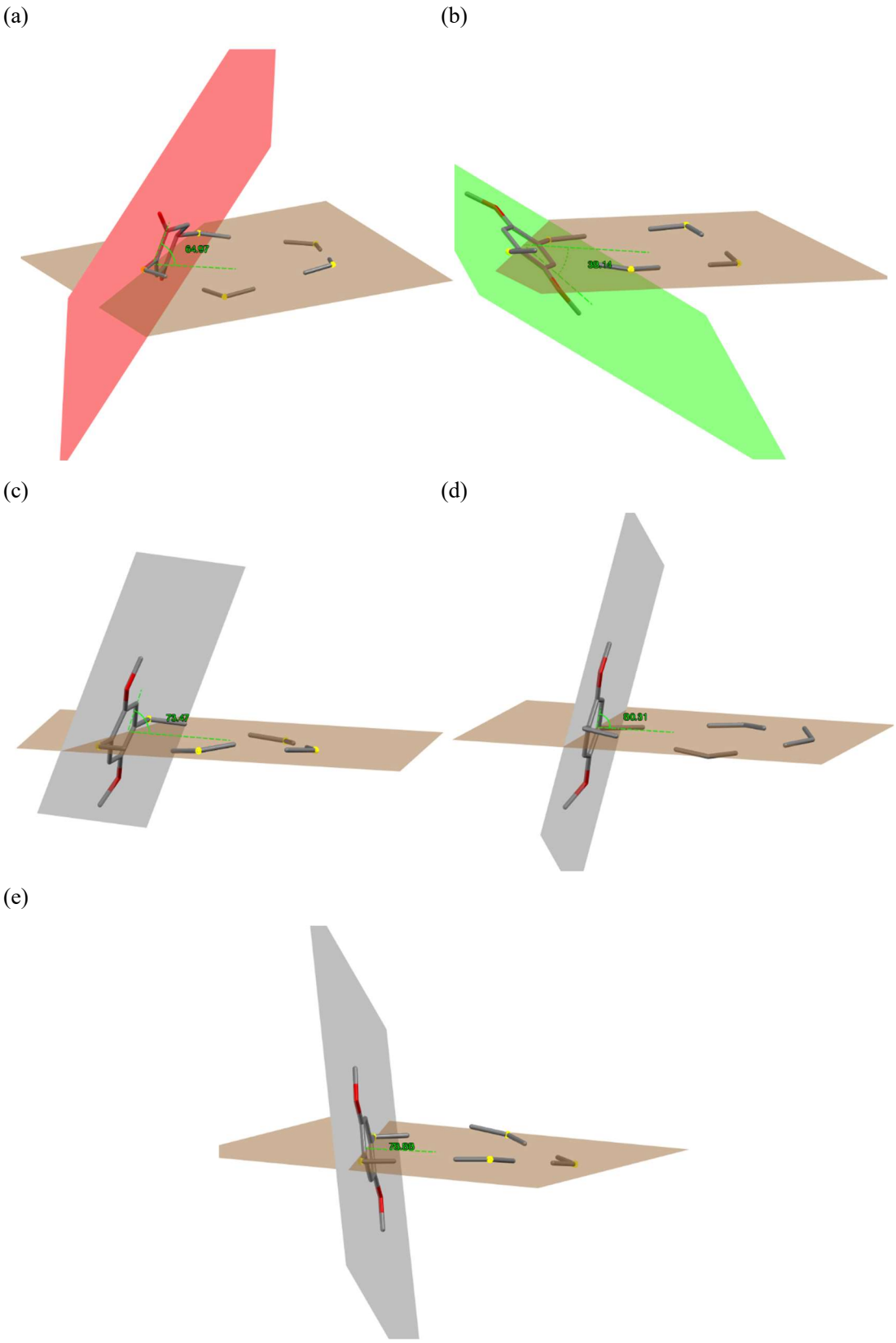

Fig. S47. Partial crystal Structures of [MeCN⊂**MeP[5]DA-1**]. (a) 1,4-dione ring A (red), (b) Ring B (green), (c) Ring C (grey), (d) Ring D (grey) and (e) Ring E (grey) form a dihedral angle of 64.97°/38.14°/73.47°/80.31°/78.88° with the bridge methylene plane (brown). The yellow atoms are methylene.

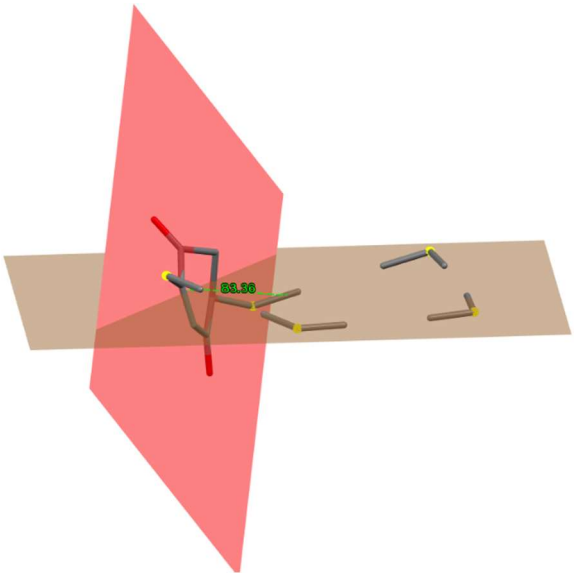

Fig. S48. Partial crystal Structures of **MeP[5]DA-2**. 1,4-dione ring A (red) form a dihedral angle of 83.36° with the bridge methylene plane (brown). The yellow atoms are methylene.

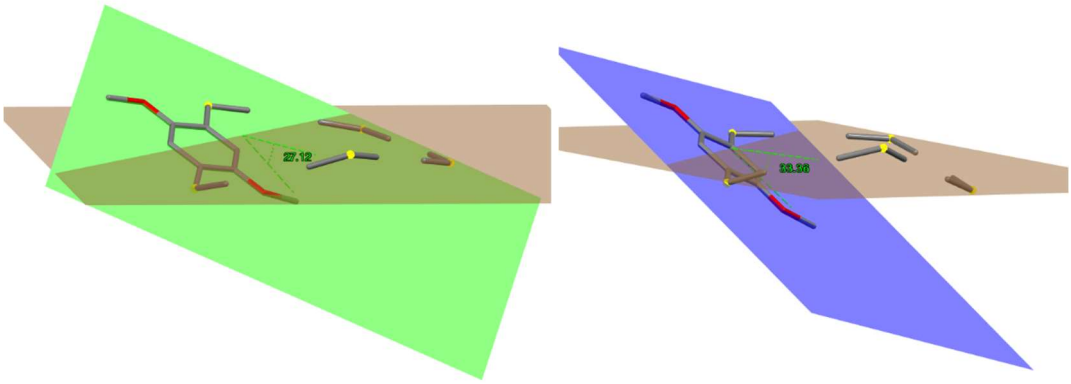

Fig. S49. Partial crystal Structures of **MeP[5]DA-2**. ring B (green)/ring E (blue) form a dihedral angle of 27.12°/33.36° with the bridge methylene plane (brown). The yellow atoms are methylene.

Table S1. Crystal data and structure refinement of **MeP[5]DA-1**.

Empirical formula	$C_{47}H_{50}O_{10}$
Formula weight	774.87
Temperature / K	159.99(10)
Crystal system	monoclinic
Space group	$P2_1/n$
a / Å	21.9521(5)
b / Å	8.76930(10)
c / Å	23.5464(6)
α / °	90
β / °	111.735(3)
γ / °	90
Volume / Å^3	4210.54(17)
Z	4
ρ_{calc} / g cm^{-3}	1.222
μ / mm^{-1}	0.085
F / 000	1648.0
2θ range for data collection / °	3.994–58.37
Crystal size / mm^3	0.2 × 0.1 × 0.1
Index ranges	$-29 \leq h \leq 28$, $-10 \leq k \leq 11$, $-32 \leq l \leq 30$
Reflections collected	51020
Independent reflections	9681 [$R_{int} = 0.0270$, $R_{sigma} = 0.0249$]
Data / restraints / parameters	9681/0/522
Goodness-of-fit on F^2	1.070
Final R indices [$I >= 2\sigma(I)$]	$R_1 = 0.0427$, $wR_2 = 0.1140$
Final R indices [all data]	$R_1 = 0.0589$, $wR_2 = 0.1218$
Largest diff. peak / hole / e Å^{-3}	0.84/-0.22
CCDC	2223646

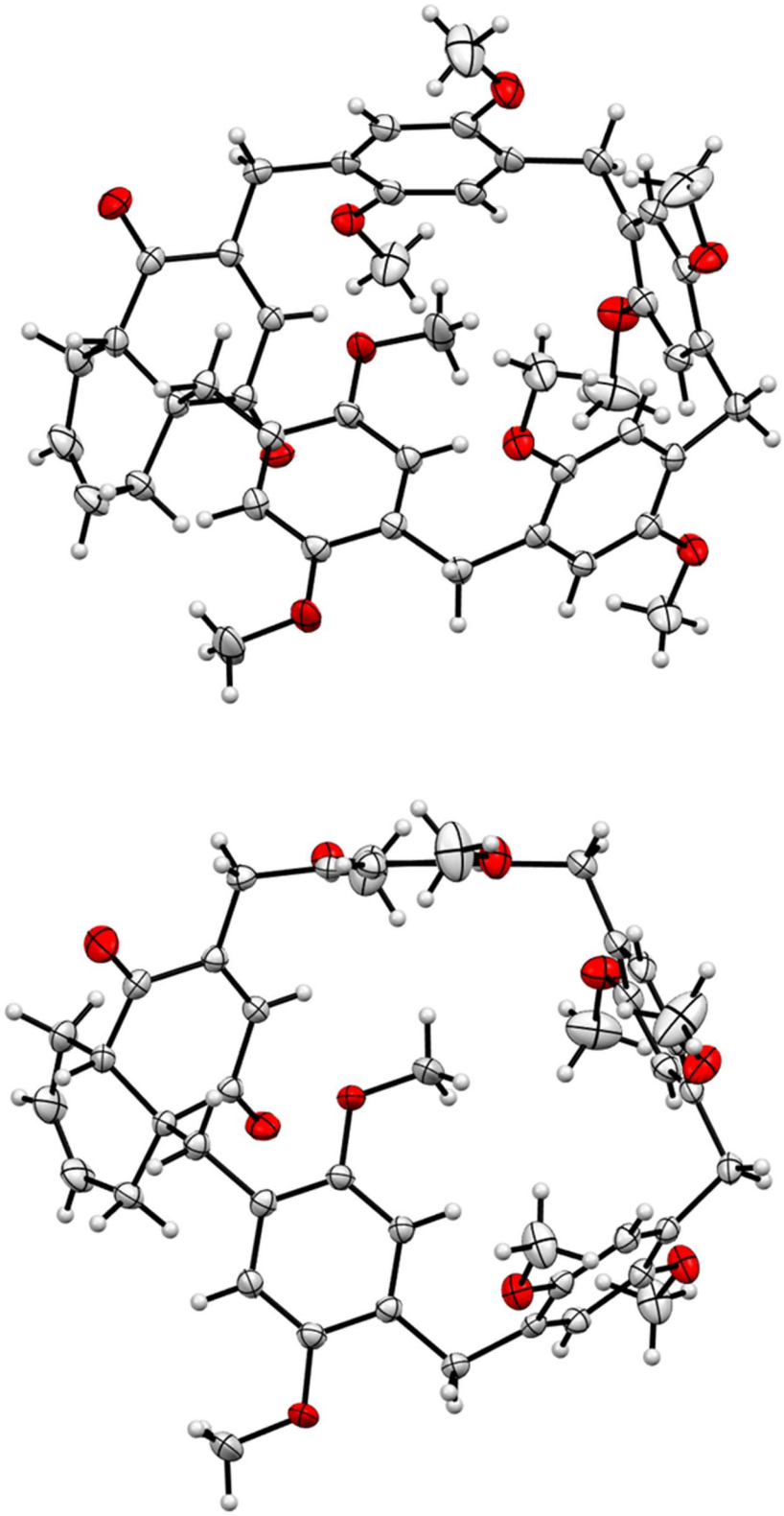

Fig. S50. Perspective ORTEP drawing of X-ray structure of **MeP[5]DA-1** (displacement ellipsoids are drawn at the 50% probability level).

Table S2. Crystal data and structure refinement of [**MeCN⊂MeP[5]DA-1**].

Empirical formula	$C_{54}H_{62}O_{10}N_2$
Formula weight / g mol^{-1}	899.05
Temperature / K	160.00(10)
Crystal system	triclinic
Space group	*P*-1
a / Å	11.5712(2)
b / Å	13.5551(3)
c / Å	17.3345(4)
α / °	107.357(2)
β / °	98.929(2)
γ / °	105.723(2)
Volume / Å^3	2414.13(9)
Z	2
ρ_{calc} / g cm^{-3}	1.237
μ / mm^{-1}	0.686
F / 000	960.0
2*θ* range for data collection / °	5.526–149.276
Crystal size / mm^3	0.2 × 0.2 × 0.2
Index ranges	$-14 \le h \le 14$, $-12 \le k \le 16$, $-21 \le l \le 20$
Reflections collected	28694
Independent reflections	9536 [R_{int} = 0.0403, R_{sigma} = 0.0426]
Data / restraints / parameters	9536/0/605
Goodness-of-fit on F^2	1.074
Final *R* indices [I >= 2σ (*I*)]	R_1 =0.0419, wR_2 = 0.1080
Final *R* indices [all data]	R_1 = 0.0536, wR_2 = 0.1179
Largest diff. peak / hole / e Å^{-3}	0.61/-0.24
CCDC	2223641

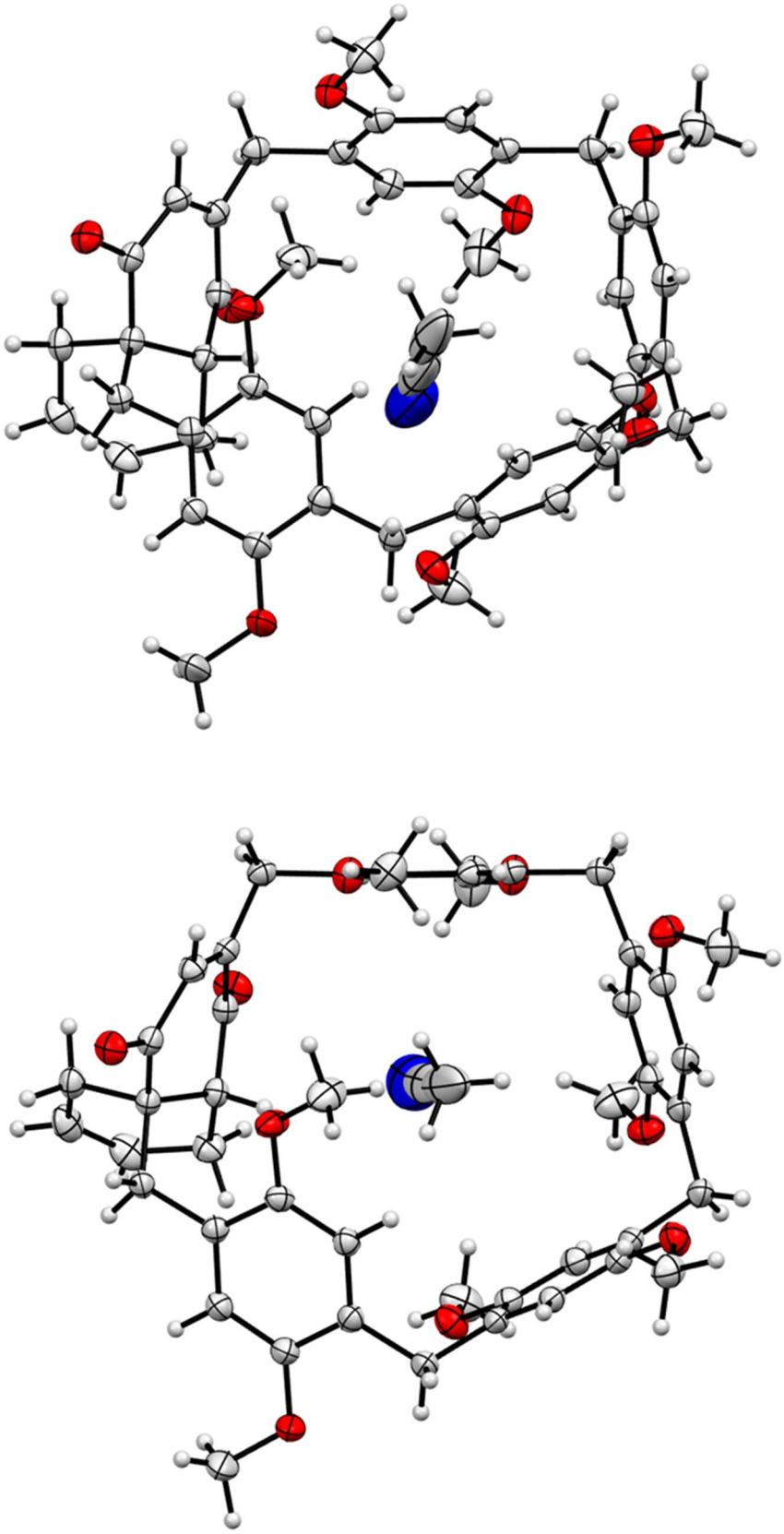

Fig. S51. Perspective ORTEP drawing of X-ray structure of [**MeCN⊂MeP[5]DA-1**] (displacement ellipsoids are drawn at the 50% probability level).

Table S3. Crystal data and structure refinement of [**MeCN⊂EtP[5]DA**].

Empirical formula	$C_{57}H_{69}O_{10}N$
Formula weight / g mol^{-1}	928.13
Temperature / K	160.01(10)
Crystal system	triclinic
Space group	*P*-1
a / Å	12.0623(3)
b / Å	13.1664(2)
c / Å	16.5167(3)
α / °	99.2010(10)
β / °	92.828(2)
γ / °	101.636(2)
Volume / Å^3	2527.12(9)
Z	2
ρ_{calc} / g cm^{-3}	1.220
μ / mm^{-1}	0.663
F / 000	996.0
2*θ* range for data collection / °	5.44–152.732
Crystal size / mm^3	0.1 × 0.1 × 0.1
Index ranges	-15 ≤ h ≤ 15, -15 ≤ k ≤ 16, -20 ≤ l ≤ 16
Reflections collected	35596
Independent reflections	10101 [R_{int} = 0.0261, R_{sigma} = 0.0238]
Data / restraints / parameters	10101/0/622
Goodness-of-fit on F^2	1.032
Final *R* indices [I >= 2σ (*I*)]	R_1 =0.0387, wR_2 = 0.0989
Final *R* indices [all data]	R_1 = 0.0425, wR_2 = 0.1012
Largest diff. peak / hole / e Å^{-3}	0.22/-0.18
CCDC	2223642

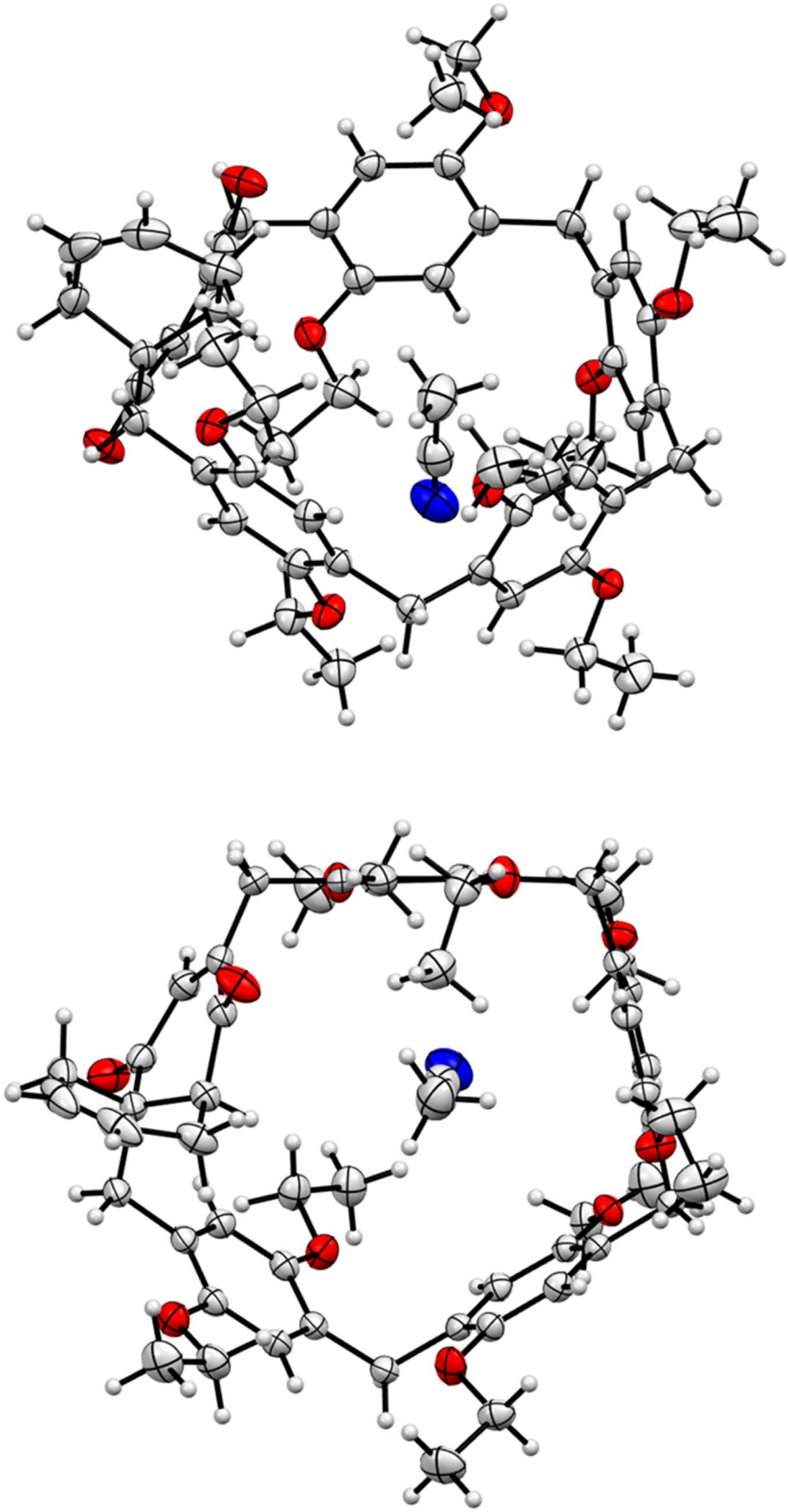

Fig. S52. Perspective ORTEP drawing of X-ray structure of [**MeCN⊂EtP[5]DA**] (displacement ellipsoids are drawn at the 50% probability level).

Table S4. Crystal data and structure refinement of **MeP[5]DA-2**.

Empirical formula	$C_{50}H_{54}O_{10}Cl_3$
Formula weight / g mol^{-1}	921.28
Temperature / K	293(2)
Crystal system	monoclinic
Space group	$P2_1/n$
a / Å	9.1056(2)
b / Å	23.9033(6)
c / Å	21.7204(6)
α / °	90
β / °	93.438(2)
γ / °	90
Volume / Å^3	4719.0(2)
Z	4
ρ_{calc} / g cm^{-3}	1.297
μ / mm^{-1}	2.228
F / 000	1940.0
2θ range for data collection / °	5.504–133.202
Crystal size / mm^3	0.3 × 0.3 × 0.1
Index ranges	-6 ≤ h ≤ 10, -27 ≤ k ≤ 28, -25 ≤ l ≤ 25
Reflections collected	36780
Independent reflections	8172 [R_{int} = 0.1169, R_{sigma} = 0.0670]
Data / restraints / parameters	8172/55/645
Goodness-of-fit on F^2	1.231
Final R indices [I >= 2σ (I)]	R_1 =0.1145, wR_2 = 0.3189
Final R indices [all data]	R_1 = 0.1413, wR_2 = 0.3406
Largest diff. peak / hole / e Å^{-3}	0.61/-0.49
CCDC	2223647

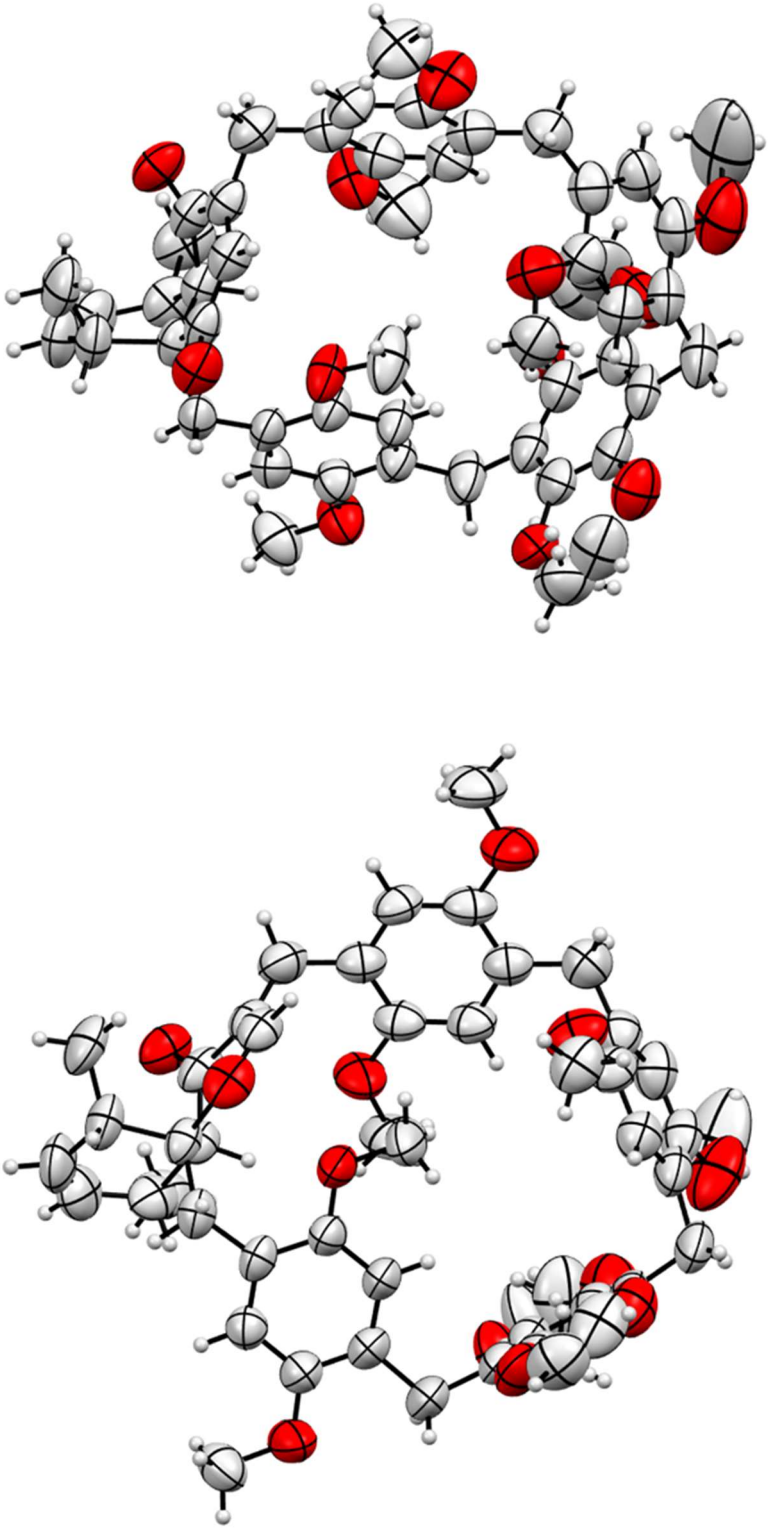

Fig. S53. Perspective ORTEP drawing of X-ray structure of **MeP[5]DA-2** (displacement ellipsoids are drawn at the 50% probability level).

Table S5. Crystal data and structure refinement of **EtP[6]DA** crystallised in MeCN.

Empirical formula	$C_{66}H_{80}O_{12}$
Formula weight / g mol^{-1}	1065.30
Temperature / K	160.00(10)
Crystal system	triclinic
Space group	*P*-1
a / Å	8.0203(6)
b / Å	26.7025(14)
c / Å	27.979(2)
α / °	75.127(6)
β / °	85.524(7)
γ / °	89.818(5)
Volume / Å^3	5772.7(7)
Z	4
ρ_{calc} / g cm^{-3}	1.226
μ / mm^{-1}	0.668
F / 000	2288.0
2θ range for data collection / °	3.424–100.868
Crystal size / mm^3	0.05 × 0.01 × 0.01
Index ranges	-4 ≤ h ≤ 8, -26 ≤ k ≤ 26, -27 ≤ l ≤ 27
Reflections collected	37108
Independent reflections	11928 [R_{int} = 0.1906, R_{sigma} = 0.2459]
Data / restraints / parameters	11928/0/1425
Goodness-of-fit on F^2	0.995
Final *R* indices [I >= 2σ (*I*)]	R_1 =0.1145, wR_2 = 0.2703
Final *R* indices [all data]	R_1 = 0.2714, wR_2 = 0.3702
Largest diff. peak / hole / e Å^{-3}	0.39/-0.32
CCDC	2223643

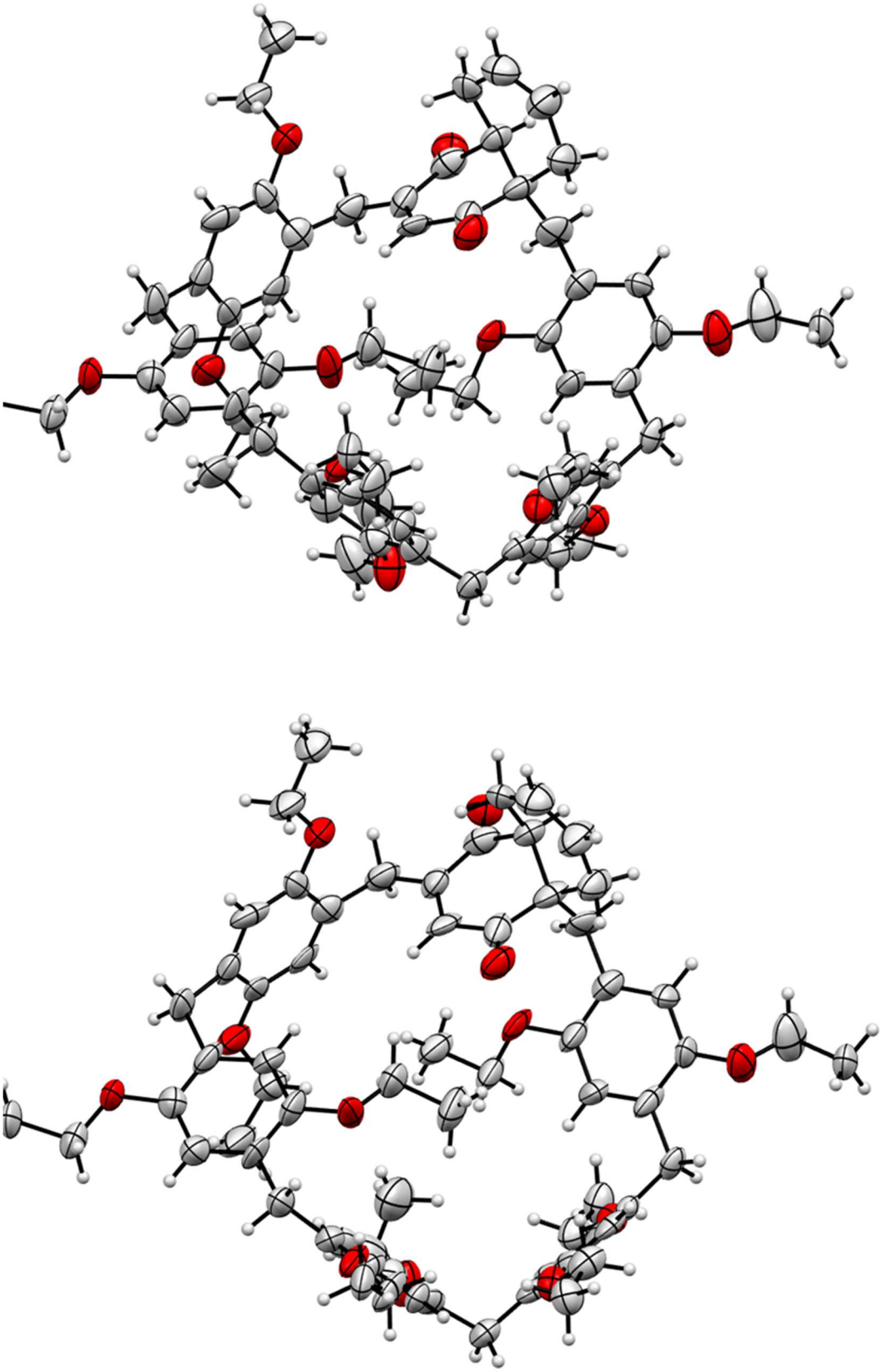

Fig. S54. Perspective ORTEP drawing of X-ray structure of **EtP[6]DA** (displacement ellipsoids are drawn at the 50% probability level).

5. Resolution of DA adducts

High-performance liquid chromatography (HPLC) analyses were operated using a LC-16A instrument (shimadzu corporation kyoto Japan). The separation was performed on a CHIRALPAK IE HPLC analytical column (5 μm, ID 4.6 mm × L 250 mm) purchased from Daicel Chemical Flow rate of the mobile phase: 0.5 mL/min; wavelength of UV-detection: 300 nm; column temperature: 25 °C; sample injection volume: 10 μL. The isolation of *rac*-**MeP[5]DA-1** was using a LC-16A instrument (shimadzu corporation kyoto Japan). The isomeric mixture (10 mg) was dissolved in 12 ml of 50 % chloroform and 50 % toluene, and then collected in a single injection by the manual operation with a 2 mL syringe and 1 mL sample loop. The separation was performed on semi-preparative column (5 μm, ID 10 mm × L 250 mm). The flow rate was 2 mL/min. The mixture was carried out using mobile phase consisting of 50 % solvent A (Chloroform) and 50 % solvent B (Toluene).

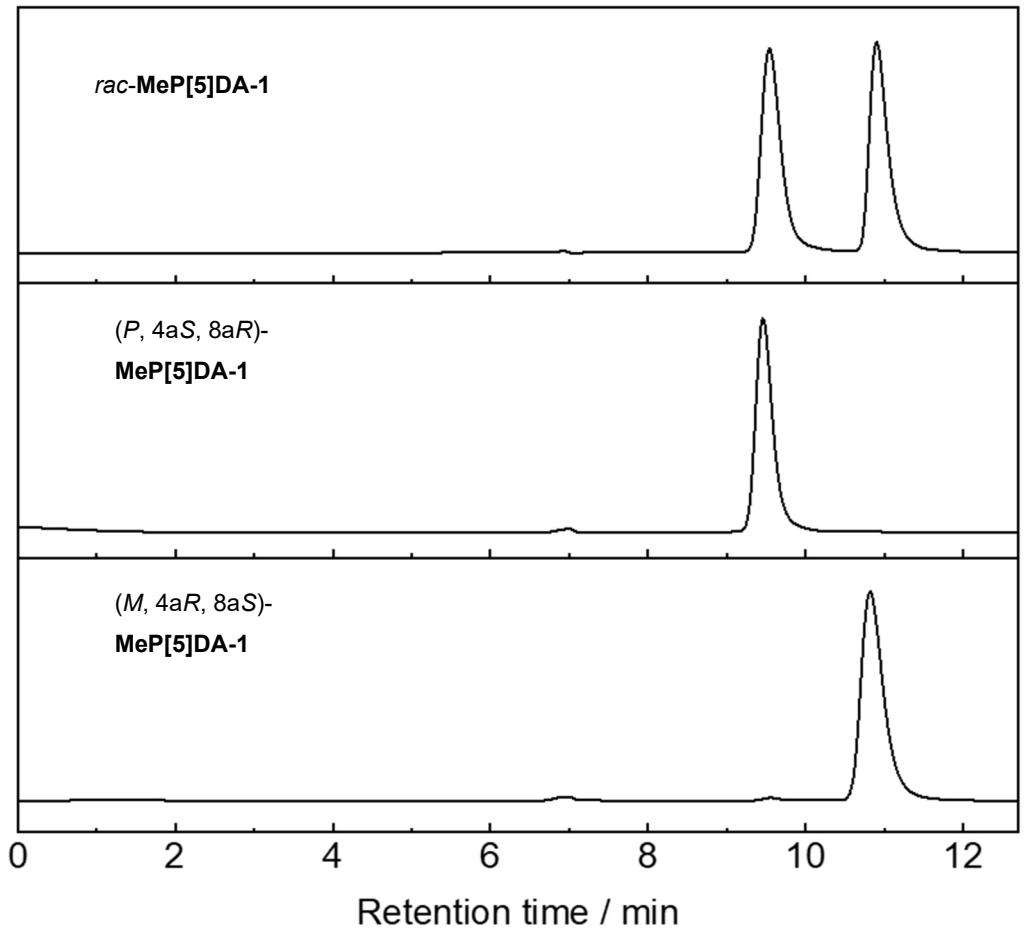

Fig. S55. Analytical HPLC chromatograms (gradient of Chloroform/Toluene, 50:50, λ = 300 nm) of samples of the resolved enantiomers (*P*, 4a*S*, 8a*R*)-**MeP[5]DA-1** (middle), (*M*, 4a*R*, 8a*S*)-**MeP[5]DA-1** (bottom) and the racemic mixture *rac*-**MeP[5]DA-1** (top).

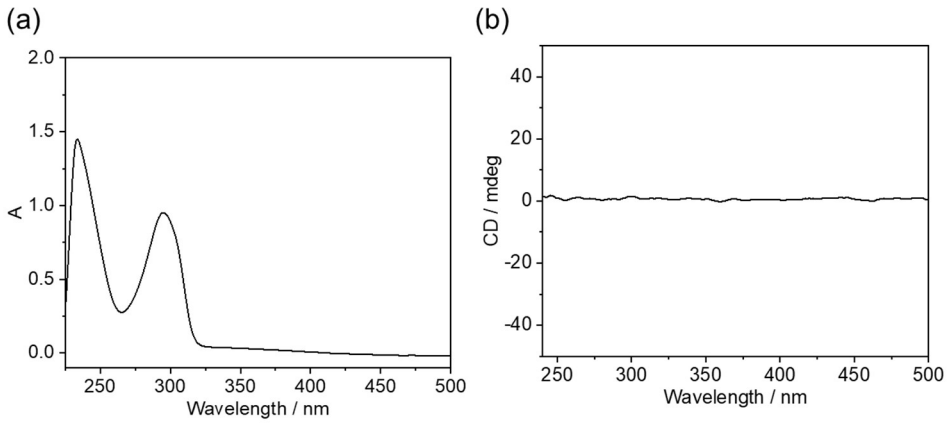

Fig. S56. (a) UV-Vis Spectrum and (b) experimental ECD spectroscopy of *rac*-**MeP[5]DA-1** recorded in CH_2Cl_2 (55 μM).

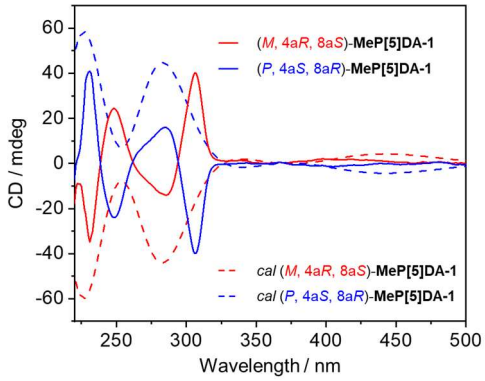

Fig. S57. Experimental and calculated ECD spectra of (*M*)-**MeP[5]DA-1** (red) and (*P*)-**MeP[5]DA-1** (blue) recorded in CH_2Cl_2 (55 μM). The initial structures were extracted from the single crystal data and optimised at DFT-D3 b3lyp/6-31+g(d,p)[8] level with solvent set of dichloromethane (CH_2Cl_2). The calculated ECD spectra were also performed in CH_2Cl_2 at TD-DFT cam-b3lyp/6-311g(d,p) level with nstates of 30.

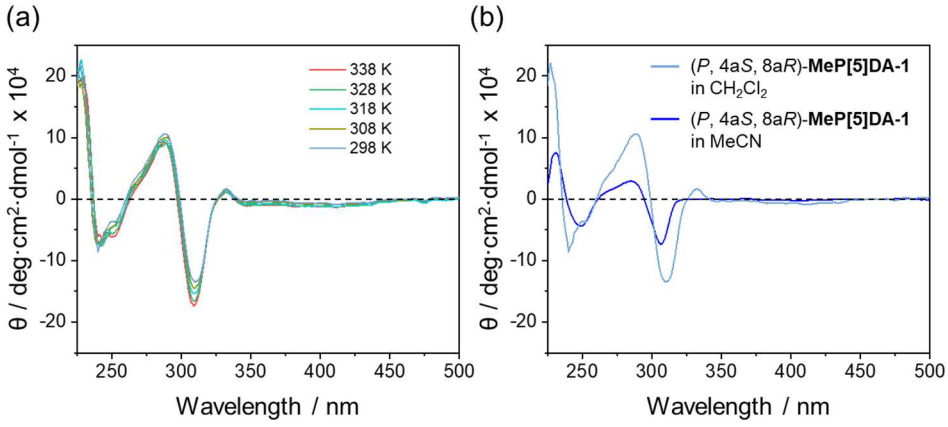

Fig. S58. (a) Variable temperature ECD spectra of (*P*)-**MeP[5]DA-1** recorded in MeCN (20 μM). (b) ECD spectra of (*P*)-**MeP[5]DA-1** recorded in CH_2Cl_2 (55 μM) and in MeCN (20 μM) at 298 K.

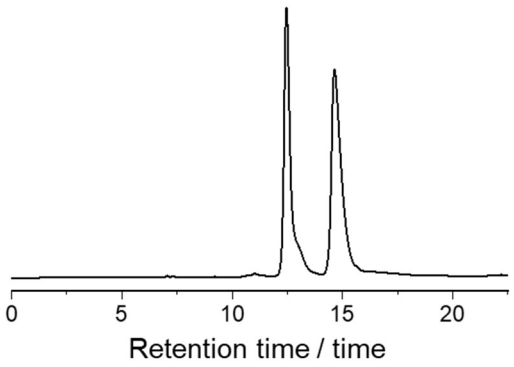

Fig. S59. HPLC chromatogram (gradient of chloroform/toluene, 20:80, λ = 300 nm) of **MeP[5]DA-2**.

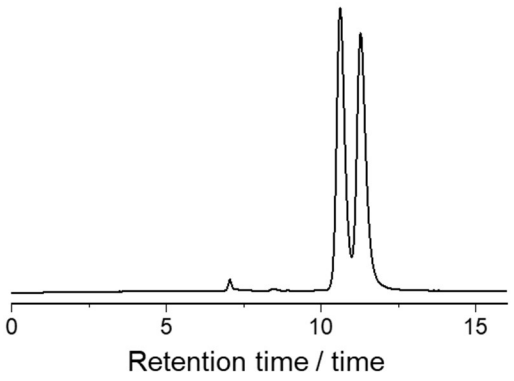

Fig. S60. HPLC chromatogram (gradient of Chloroform/Toluene, 10:90, λ = 300 nm) of **EtP[5]DA**.

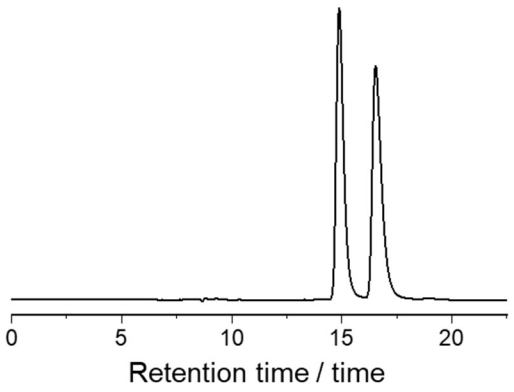

Fig. S61. HPLC chromatogram (gradient of Chloroform/*n*-hexane, 60:40, λ = 300 nm) of **EtP[6]DA**.

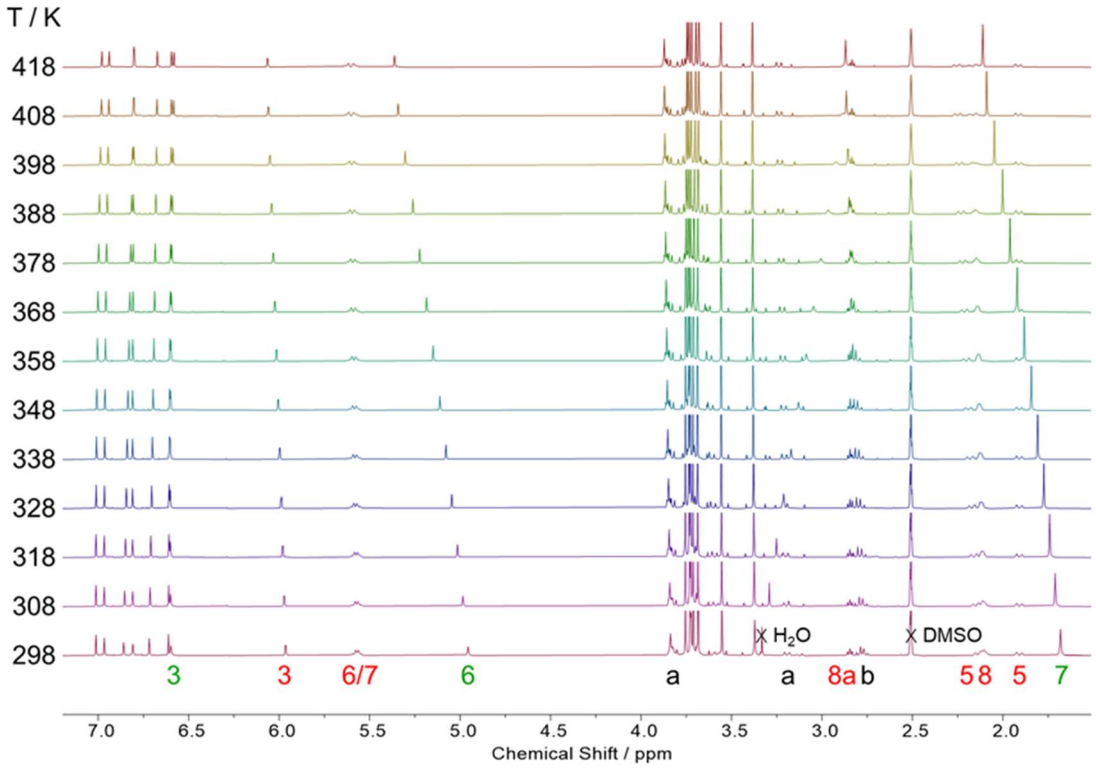

Fig. S62. Variable temperature NMR spectra of **MeP[5]DA-1** recorded in DMSO-d_6 from 298 K to 418 K.

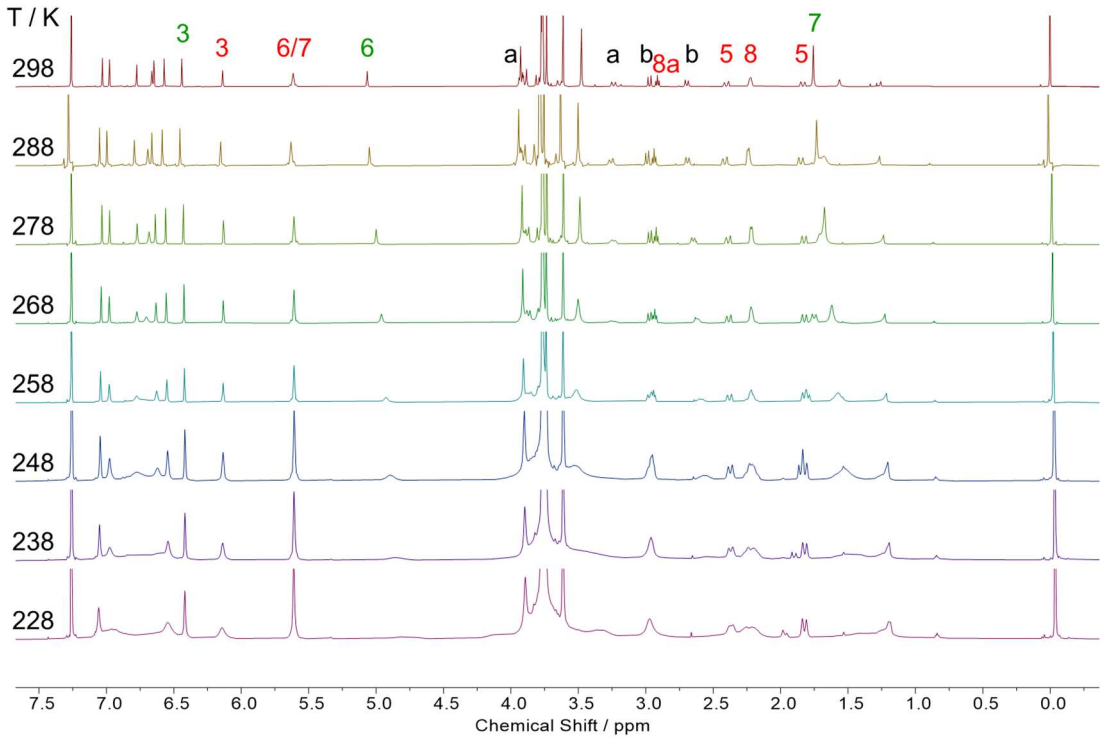

Fig. S63. Variable temperature NMR spectra of **MeP[5]DA-1** recorded in $CDCl_3$ from 228 K to 298 K.

6. Reference

1. Dolomanov, O. V.; Bourhis, L. J.; Gildea, R. J.; Howarda J. A. K.; Puschmann, H. *J*, *Appl*. *Cryst*. **2009**, *42*, 339–341.
2. Sheldrick, G. M. *Acta Cryst. Sect*. **2008**, *64*, 112–122.
3. Han, C.; Zhang, Z.; Yu, G.; Huang, F. *Chem. Commun*. **2012**, *48*, 9876–9878.
4. Kou, Y.; Cao, D.; Tao, H.; Wang, L.; Liang, J.; Chen, Z.; Meier, H. *J*. *Incl*. *Phenom*. *Macrocycl*. *Chem*. **2013**, *77*, 279–289.
5. Wu, X.; Chen, Y.; Hu, W.; Liu, Y.; Jia, X.; Li, J.; Jiang, B.; Wen, K. *Org*. *Biomol*. *Chem*. **2017**,*15*, 4897–4900.
6. Cao, J.; Shang, Y.; Qi, B.; Sun, X.; Zhang, L.; Liu, H.; Zhang, H.; Zhou, X. *RSC Adv*. **2015**, *5*, 9993–9996.
7. Avei, M. R.; Etezadi, S.; Captain, B.; Kaifer, A. E. *Commun*. *Chem*. **2020**, *3*, 117–131.
8. Gaussian 09, Revision D.01, M. J. Frisch, G. W. Trucks, H. B. Schlegel, G. E. Scuseria, M. A. Robb, J. R. Cheeseman, G. Scalmani, V. Barone, B. Mennucci, G. A. Petersson, H. Nakatsuji, M. Caricato, X. Li, H. P. Hratchian, A. F. Izmaylov, J. Bloino, G. Zheng, J. L. Sonnenberg, M. Hada, M. Ehara, K. Toyota, R. Fukuda, J. Hasegawa, M. Ishida, T. Nakajima, Y. Honda, O. Kitao, H. Nakai, T. Vreven, J. A. Montgomery, Jr., J. E. Peralta, F. Ogliaro, M. Bearpark, J. J. Heyd, E. Brothers, K. N. Kudin, V. N. Staroverov, T. Keith, R. Kobayashi, J. Normand, K. Raghavachari, A. Rendell, J. C. Burant, S. S. Iyengar, J. Tomasi, M. Cossi, N. Rega, J. M. Millam, M. Klene, J. E. Knox, J. B. Cross, V. Bakken, C. Adamo, J. Jaramillo, R. Gomperts, R. E. Stratmann, O. Yazyev, A. J. Austin, R. Cammi, C. Pomelli, J. W. Ochterski, R. L. Martin, K. Morokuma, V. G. Zakrzewski, G. A. Voth, P. Salvador, J. J. Dannenberg, S. Dapprich, A. D. Daniels, O. Farkas, J. B. Foresman, J. V. Ortiz, J. Cioslowski, and D. J. Fox, Gaussian, Inc., Wallingford CT, 2013.